Haus, Hermann A., and James R. Melcher. *Electromagnetic Fields and Energy.* Englewood Cliffs, NJ: Prentice-Hall, 1989. ISBN: 9780132490207.

7

CONDUCTION AND ELECTROQUASISTATIC CHARGE RELAXATION

7.0 INTRODUCTION

This is the last in the sequence of chapters concerned largely with electrostatic and electroquasistatic fields. The electric field $\mathbf{E}$ is still irrotational and can therefore be represented in terms of the electric potential Φ.

$$\boxed{\nabla \times \mathbf{E} = 0 \Leftrightarrow \mathbf{E} = -\nabla\Phi} \tag{1}$$

The source of $\mathbf{E}$ is the charge density. In Chap. 4, we began our exploration of EQS fields by treating the distribution of this source as prescribed. By the end of Chap. 4, we identified solutions to boundary value problems, where equipotential surfaces were replaced by perfectly conducting metallic electrodes. There, and throughout Chap. 5, the sources residing on the surfaces of electrodes as surface charge densities were made self-consistent with the field. However, in the volume, the charge density was still prescribed.

In Chap. 6, the first of two steps were taken toward a self-consistent description of the charge density in the volume. In relating $\mathbf{E}$ to its sources through Gauss' law, we recognized the existence of two types of charge densities, ρ_u and ρ_p, which, respectively, represented unpaired and paired charges. The paired charges were related to the polarization density $\mathbf{P}$ with the result that Gauss' law could be written as (6.2.15)

$$\boxed{\nabla \cdot \mathbf{D} = \rho_u} \tag{2}$$

where $\mathbf{D} \equiv \epsilon_o\mathbf{E} + \mathbf{P}$. Throughout Chap. 6, the volume was assumed to be perfectly insulating. Thus, ρ_p was either zero or a given distribution.

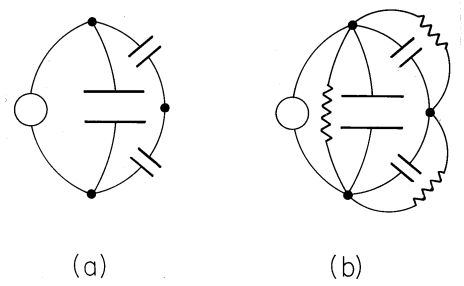

Fig. 7.0.1 EQS distributions of potential and current density are analogous to those of voltage and current in a network of resistors and capacitors. (a) Systems of perfect dielectrics and perfect conductors are analogous to capacitive networks. (b) Conduction effects considered in this chapter are analogous to those introduced by adding resistors to the network.

The second step toward a self-consistent description of the volume charge density is taken by adding to (1) and (2) an equation expressing conservation of the unpaired charges, (2.3.3).

$$\boxed{\nabla \cdot \mathbf{J}_u + \frac{\partial \rho_u}{\partial t} = 0} \tag{3}$$

That the charge appearing in this equation is indeed the unpaired charge density follows by taking the divergence of Ampère's law expressed with polarization, (6.2.17), and using Gauss' law as given by (2) to eliminate $\mathbf{D}$.

To make use of these three differential laws, it is necessary to specify $\mathbf{P}$ and $\mathbf{J}$. In Chap. 6, we learned that the former was usually accomplished by either specifying the polarization density $\mathbf{P}$ or by introducing a polarization constitutive law relating $\mathbf{P}$ to $\mathbf{E}$. In this chapter, we will almost always be concerned with linear dielectrics, where $\mathbf{D} = \epsilon\mathbf{E}$.

A new constitutive law is required to relate $\mathbf{J}_u$ to the electric field intensity. The first of the following sections is therefore devoted to the constitutive law of conduction. With the completion of Sec. 7.1, we have before us the differential laws that are the theme of this chapter.

To anticipate the developments that follow, it is helpful to make an analogy to circuit theory. If the previous two chapters are regarded as describing circuits consisting of interconnected capacitors, as shown in Fig. 7.0.1a, then this chapter adds resistors to the circuit, as in Fig. 7.0.1b. Suppose that the voltage source is a step function. As the circuit is composed of resistors and capacitors, the distribution of currents and voltages in the circuit is finally determined by the resistors alone. That is, as $t \to \infty$, the capacitors cease charging and are equivalent to open circuits. The distribution of voltages is then determined by the steady flow of current through the resistors. In this long-time limit, the charge on the capacitors is determined from the voltages already specified by the resistive network.

The steady current flow is analogous to the field situation where $\partial\rho_u/\partial t \to 0$ in the conservation of charge expression, (3). We will find that (1) and (3), the latter written with $\mathbf{J}_u$ represented by the conduction constitutive law, then fully determine the distribution of potential, of $\mathbf{E}$, and hence of $\mathbf{J}_u$. Just as the charges

on the capacitors in the circuit of Fig. 7.0.1b are then specified by the already determined voltage distribution, the charge distribution can be found in an after-the-fact fashion from the already determined field distribution by using Gauss' law, (2). After considering the physical basis for common conduction constitutive laws in Sec. 7.1, Secs. 7.2–7.6 are devoted to steady conduction phenomena.

In the circuit of Fig. 7.0.1b, the distribution of voltages an instant after the voltage step is applied is determined by the capacitors without regard for the resistors. From a field theory point of view, this is the physical situation described in Chaps. 4 and 5. It is the objective of Secs. 7.7–7.9 to form an appreciation for how this initial distribution of the fields and sources relaxes to the steady condition, already studied in Secs. 7.2–7.6, that prevails when $t \to \infty$.

In Chaps. 3–5 we invoked the "perfect conductivity" model for a conductor. For electroquasistatic systems, we will conclude this chapter with an answer to the question, "Under what circumstances can a conductor be regarded as perfect?"

Finally, if the fields and currents are essentially static, there is no distinction between EQS and MQS laws. That is, if $\partial \mathbf{B}/\partial t$ is negligible in an MQS system, Faraday's law again reduces to (1). Thus, the first half of this chapter provides an understanding of steady conduction in some MQS as well as EQS systems. In Chap. 8, we determine the magnetic field intensity from a given distribution of current density. Provided that rates of change are slow enough so that effects of magnetic induction can be ignored, the solution to the steady conduction problem as addressed in Secs. 7.2–7.6 provides the distribution of the magnetic field source, the current density, needed to begin Chap. 8.

Just how fast can the fields vary without producing effects of magnetic induction? For EQS systems, the answer to this question comes in Secs. 7.7–7.9. The EQS effects of finite conductivity and finite rates of change are in sharp contrast to their MQS counterparts, studied in the last half of Chap. 10.

7.1 CONDUCTION CONSTITUTIVE LAWS

In the presence of materials, fields vary in space over at least two length scales. The *microscopic scale* is typically the distance between atoms or molecules while the much larger *macroscopic scale* is typically the dimension of an object made from the material. As developed in the previous chapter, fields in polarized media are averages over the microscopic scale of the dipoles. In effect, the experimental determination of the polarization constitutive law relating the macroscopic $\mathbf{P}$ and $\mathbf{E}$ (Sec. 6.4) does not deal with the microscopic field.

With the understanding that experimentally measured values will again be used to evaluate macroscopic parameters, we assume that the average force acting on an unpaired or free charge, q, within matter is of the same form as the Lorentz force, (1.1.1).

$$\mathbf{f} = q(\mathbf{E} + \mathbf{v} \times \mu_o \mathbf{H}) \tag{1}$$

By contrast with a polarization charge, a free charge is not bound to the atoms and molecules, of which matter is constituted, but under the influence of the electric and magnetic fields can travel over distances that are large compared to interatomic or intermolecular distances. In general, the charged particles collide with the atomic

or molecular constituents, and so the force given by (1) does not lead to uniform acceleration, as it would for a charged particle in free space. In fact, in the conventional conduction process, a particle experiences so many collisions on time scales of interest that the average velocity it acquires is quite low. This phenomenon gives rise to two consequences. First, inertial effects can be disregarded in the time average balance of forces on the particle. Second, the velocity is so low that the forces due to magnetic fields are usually negligible. (The magnetic force term leads to the Hall effect, which is small and very difficult to observe in metallic conductors, but because of the relatively larger translational velocities reached by the charge carriers in semiconductors, more easily observed in these.)

With the driving force ascribed solely to the electric field and counterbalanced by a "viscous" force, proportional to the average translational velocity $\mathbf{v}$ of the charged particle, the force equation becomes

$$\mathbf{f} = \pm|q_\pm|\mathbf{E} = \nu_\pm \mathbf{v} \tag{2}$$

where the upper and lower signs correspond to particles of positive and negative charge, respectively. The coefficients $\nu_\pm$ are positive constants representing the time average "drag" resulting from collisions of the carriers with the fixed atoms or molecules through which they move.

Written in terms of the *mobilities*, $\mu_\pm$, the velocities of the positive and negative particles follow from (2) as

$$\mathbf{v}_\pm = \pm\mu_\pm \mathbf{E} \tag{3}$$

where $\mu_\pm = |q_\pm|/\nu_\pm$. The mobility is defined as positive. The positive and negative particles move with and against the electric field intensity, respectively.

Now suppose that there are two types of charged particles, one positive and the other negative. These might be the positive sodium and negative chlorine ions resulting when salt is dissolved in water. In a metal, the positive charges represent the (zero mobility) atomic sites, while the negative particles are electrons. Then, with N_+ and N_-, respectively, defined as the number of these charged particles per unit volume, the current density is

$$\mathbf{J}_u = N_+|q_+|\mathbf{v}_+ - N_-|q_-|\mathbf{v}_- \tag{4}$$

A flux of negative particles comprises an electrical current that is in a direction opposite to that of the particle motion. Thus, the second term in (4) appears with a negative sign. The velocities in this expression are related to $\mathbf{E}$ by (3), so it follows that the current density is

$$\mathbf{J}_u = (N_+|q_+|\mu_+ + N_-|q_-|\mu_-)\mathbf{E} \tag{5}$$

In terms of the same variables, the unpaired charge density is

$$\rho_u = N_+|q_+| - N_-|q_-| \tag{6}$$

Ohmic Conduction. In general, the distributions of particle densities N_+ and N_- are determined by the electric field. However, in many materials, the quantity in brackets in (5) is a property of the material, called the *electrical conductivity* σ.

$$\boxed{\mathbf{J}_u = \sigma\mathbf{E}; \qquad \sigma \equiv (N_+|q_+|\mu_+ + N_-|q_-|\mu_-)} \tag{7}$$

The MKS units of σ are (ohm - m)$^{-1}$ $\equiv$ Siemens/m = S/m.

In these materials, the charge densities N_+q_+ and N_-q_- keep each other in (approximate) balance so that there is little effect of the applied field on their sum. Thus, the conductivity $\sigma(\mathbf{r})$ is specified as a function of position in nonuniform media by the distribution $N_\pm$ in the material and by the local mobilities, which can also be functions of $\mathbf{r}$.

The conduction constitutive law given by (7) is *Ohm's law* generalized in a field-theoretical sense. Values of the conductivity for some common materials are given in Table 7.1.1. It is important to keep in mind that any constitutive law is of restricted use, and Ohm's law is no exception. For metals and semiconductors, it is usually a good model on a sufficiently large scale. It is also widely used in dealing with electrolytes. However, as materials become semi-insulators, it can be of questionable validity.

Unipolar Conduction. To form an appreciation for the implications of Ohm's law, it will be helpful to contrast it with the law for *unipolar conduction*. In that case, charged particles of only one sign move in a neutral background, so that the expressions for the current density and charge density that replace (5) and (6) are

$$\boxed{\mathbf{J}_u = |\rho|\mu\mathbf{E}} \tag{8}$$

$$\rho_u = \rho \tag{9}$$

where the charge density ρ now carries its own sign. Typical of situations described by these relations is the passage of ions through air.

Note that a current density exists in unipolar conduction only if there is a *net* charge density. By contrast, for Ohmic conduction, where the current density and the charge density are given by (7) and (6), respectively, there can be a current density at a location where there is no *net* charge density. For example, in a metal, negative electrons move through a background of fixed positively charged atoms. Thus, in (7), $\mu_+ = 0$ and the conductivity is due solely to the electrons. But it follows from (6) that the positive charges do have an important effect, in that they can nullify the charge density of the electrons. We will often find that in an Ohmic conductor there is a current density where there is no net unpaired charge density.

7.2 STEADY OHMIC CONDUCTION

To set the stage for the next two sections, consider the fields in a material that has a linear polarizability and is described by Ohm's law, (7.1.7).

$$\boxed{\mathbf{J} = \sigma(\mathbf{r})\mathbf{E}; \qquad \mathbf{D} = \epsilon(\mathbf{r})\mathbf{E}} \tag{1}$$

TABLE 7.1.1
CONDUCTIVITY OF VARIOUS MATERIALS

Metals and Alloys in Solid State	
	$\sigma-$ mhos/m at 20°C
Aluminum, commercial hard drawn	3.54×10^7
Copper, annealed	5.80×10^7
Copper, hard drawn	5.65×10^7
Gold, pure drawn	4.10×10^7
Iron, 99.98%	1.0×10^7
Steel	$0.5–1.0 \times 10^7$
Lead	0.48×10^7
Magnesium	2.17×10^7
Nichrome	0.10×10^7
Nickel	1.28×10^7
Silver, 99.98%	6.14×10^7
Tungsten	1.81×10^7
Semi-insulating and Dielectric Solids	
Bakelite (average range)*	$10^{-8} - 10^{10}$
Celluloid*	10^{-8}
Glass, ordinary*	10^{-12}
Hard rubber*	$10^{-14} - 10^{-16}$
Mica*	$10^{-11} - 10^{-15}$
Paraffin*	$10^{-14} - 10^{-16}$
Quartz, fused*	less than 10^{-17}
Sulfur*	less than 10^{-16}
Teflon*	less than 10^{-16}
Liquids	
Mercury	0.10×10^7
Alcohol, ethyl, 15° C	3.3×10^{-4}
Water, Distilled, 18° C	2×10^{-4}
Corn Oil	5×10^{-11}

*For highly insulating materials. Ohm's law is of dubious validity and conductivity values are only useful for making estimates.

In general, these properties are functions of position, **r**. Typically, electrodes are used to constrain the potential over some of the surface enclosing this material, as suggested by Fig. 7.2.1.

In this section, we suppose that the excitations are essentially constant in

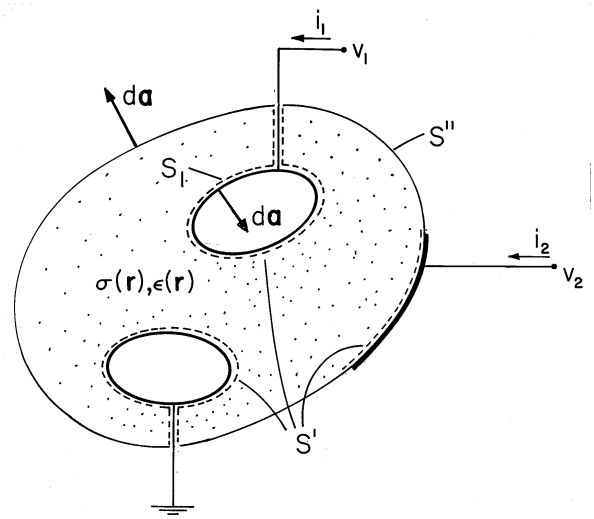

Fig. 7.2.1 Configuration having volume enclosed by surfaces S', upon which the potential is constrained, and S'', upon which its normal derivative is constrained.

time, in the sense that the rate of accumulation of charge at any given location has a negligible influence on the distribution of the current density. Thus, the time derivative of the unpaired charge density in the charge conservation law, (7.0.3), is negligible. This implies that the current density is solenoidal.

$$\boxed{\nabla \cdot \sigma \mathbf{E} = 0} \tag{2}$$

Of course, in the EQS approximation, the electric field is also irrotational.

$$\nabla \times \mathbf{E} = 0 \Leftrightarrow \mathbf{E} = -\nabla \Phi \tag{3}$$

Combining (2) and (3) gives a second-order differential equation for the potential distribution.

$$\nabla \cdot \sigma \nabla \Phi = 0 \tag{4}$$

In regions of uniform conductivity (σ = constant), it assumes a familiar form.

$$\nabla^2 \Phi = 0 \tag{5}$$

In a uniform conductor, the potential distribution satisfies Laplace's equation.

It is important to realize that the physical reasons for obtaining Laplace's equation for the potential distribution in a uniform conductor are quite different from those that led to Laplace's equation in the electroquasistatic cases of Chaps. 4 and 5. With steady conduction, the governing requirement is that the divergence of the current density vanish. The unpaired charge density does not influence the current distribution, but is rather determined by it. In a uniform conductor, the continuity constraint on **J** happens to imply that there is no unpaired charge density.

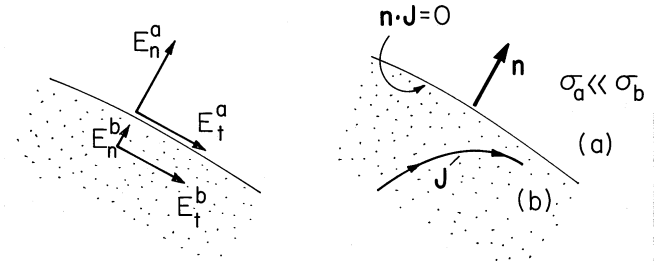

Fig. 7.2.2 Boundary between region (a) that is insulating relative to region (b).

In a nonuniform conductor, (4) shows that there is an accumulation of unpaired charge. Indeed, with σ a function of position, (2) becomes

$$\sigma \nabla \cdot \mathbf{E} + \mathbf{E} \cdot \nabla \sigma = 0 \tag{6}$$

Once the potential distribution has been found, Gauss' law can be used to determine the distribution of unpaired charge density.

$$\rho_u = \epsilon \nabla \cdot \mathbf{E} + \mathbf{E} \cdot \nabla \epsilon \tag{7}$$

Equation (6) can be solved for $div\,\mathbf{E}$ and that quantity substituted into (7) to obtain

$$\boxed{\rho_u = -\frac{\epsilon}{\sigma}\mathbf{E} \cdot \nabla \sigma + \mathbf{E} \cdot \nabla \epsilon} \tag{8}$$

Even though the distribution of ϵ plays no part in determining $\mathbf{E}$, through Gauss' law, it does influence the distribution of unpaired charge density.

Continuity Conditions. Where the conductivity changes abruptly, the continuity conditions follow from (2) and (3). The condition

$$\boxed{\mathbf{n} \cdot (\sigma_a \mathbf{E}^a - \sigma_b \mathbf{E}^b) = 0} \tag{9}$$

is derived from (2), just as (1.3.17) followed from Gauss' law. The continuity conditions implied by (3) are familiar from Sec. 5.3.

$$\boxed{\mathbf{n} \times (\mathbf{E}^a - \mathbf{E}^b) = 0 \Leftrightarrow \Phi^a - \Phi^b = 0} \tag{10}$$

Illustration. Boundary Condition at an Insulating Surface

Insulated wires and ordinary resistors are examples where a conducting medium is bounded by one that is essentially insulating. What boundary condition should be used to determine the current distribution inside the conducting material?

In Fig. 7.2.2, region (a) is relatively insulating compared to region (b), $\sigma_a \ll \sigma_b$. It follows from (9) that the normal electric field in region (a) is much greater than in region (b), $E_n^a \gg E_n^b$. According to (10), the tangential components of $\mathbf{E}$ are equal, $E_t^a = E_t^b$. With the assumption that the normal and tangential components of $\mathbf{E}$ are of the same order of magnitude in the insulating region, these two statements establish the relative magnitudes of the normal and tangential components of $\mathbf{E}$, respectively, sketched in Fig. 7.2.2. We conclude that in the relatively conducting region (b), the normal component of $\mathbf{E}$ is essentially zero compared to the tangential component. Thus, to determine the fields in the relatively conducting region, the boundary condition used *at an insulating surface* is

$$\boxed{\mathbf{n} \cdot \mathbf{J} = 0 \Rightarrow \mathbf{n} \cdot \nabla \Phi = 0} \tag{11}$$

At an insulating boundary, inside the conductor, the normal derivative of the potential is zero, while the boundary potential adjusts itself to make this true. Current lines are diverted so that they remain tangential to the insulating boundary, as sketched in Fig. 7.2.2.

Just as Gauss' law embodied in (8) is used to find the unpaired volume charge density *ex post facto*, Gauss' continuity condition (6.5.3) serves to evaluate the unpaired surface charge density. Combined with the current continuity condition, (9), it becomes

$$\boxed{\sigma_{su} = \mathbf{n} \cdot \epsilon_a \mathbf{E}^a \left(1 - \frac{\epsilon_b}{\epsilon_a} \frac{\sigma_a}{\sigma_b}\right)} \tag{12}$$

Conductance. If there are only two electrodes contacting the conductor of Fig. 7.2.1 and hence one voltage $v_1 = v$ and current $i_1 = i$, the voltage-current relation for the terminal pair is of the form

$$i = Gv \tag{13}$$

where G is the conductance. To relate G to field quantities, (2) is integrated over a volume V enclosed by a surface S, and Gauss' theorem is used to convert the volume integral to one of the current $\sigma \mathbf{E} \cdot d\mathbf{a}$ over the surface S. This integral law is then applied to the surface shown in Fig. 7.2.1 enclosing the electrode that is connected to the positive terminal. Where it intersects the wire, the contribution is $-i$, so that the integral over the closed surface becomes

$$-i + \int_{S_1} \sigma \mathbf{E} \cdot d\mathbf{a} = 0 \tag{14}$$

where S_1 is the surface where the perfectly conducting electrode having potential v_1 interfaces with the Ohmic conductor.

Division of (14) by the terminal voltage v gives an expression for the conductance defined by (13).

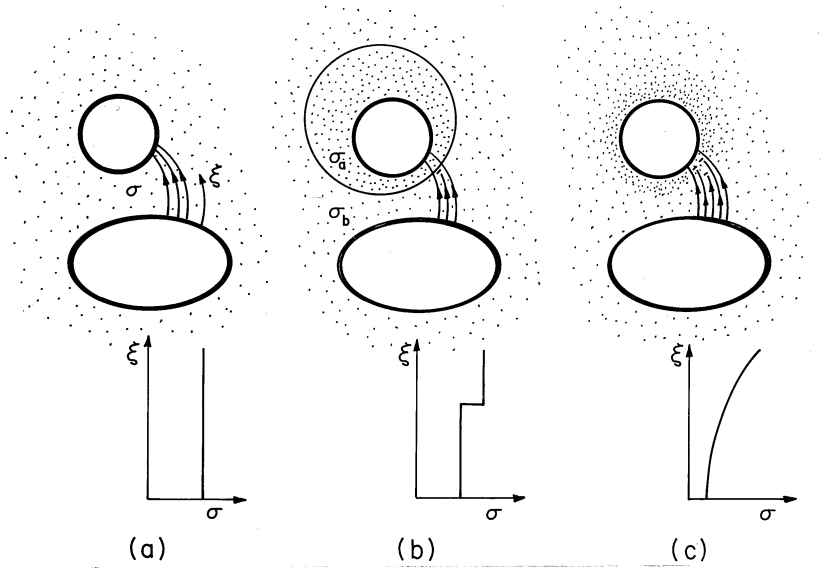

Fig. 7.2.3 Typical configurations involving a conducting material and perfectly conducting electrodes. (a) Region of interest is filled by material having uniform conductivity. (b) Region composed of different materials, each having uniform conductivity. Conductivity is discontinuous at interfaces. (c) Conductivity is smoothly varying.

$$\boxed{G = \frac{i}{v} = \frac{\int_{S_1} \sigma \mathbf{E} \cdot d\mathbf{a}}{v}} \tag{15}$$

Note that the linearity of the equation governing the potential distribution, (4), assures that i is proportional to v. Hence, (15) is independent of v and, indeed, a parameter characterizing the system independent of the excitation.

A comparison of (15) for the conductance with (6.5.6) for the capacitance suggests an analogy that will be developed in Sec. 7.5.

Qualitative View of Fields in Conductors. Three classes of steady conduction configurations are typified in Fig. 7.2.3. In the first, the region of interest is one of uniform conductivity bounded either by surfaces with constrained potentials or by perfect insulators. In the second, the conductivity varies abruptly but by a finite amount at interfaces, while in the third, it varies smoothly. Because Gauss' law plays no role in determining the potential distribution, the permittivity distributions in these three classes of configurations are arbitrary. Of course, they do have a strong influence on the resulting distributions of unpaired charge density.

A qualitative picture of the electric field distribution within conductors emerges from arguments similar to those used in Sec. 6.5 for linear dielectrics. Because $\mathbf{J}$ is solenoidal and has the same direction as $\mathbf{E}$, it passes from the high-potential to the low-potential electrodes through tubes within which lines of $\mathbf{J}$ neither terminate nor originate. The $\mathbf{E}$ lines form the same tubes but either terminate or originate on

the sum of unpaired and polarization charges. The sum of these charge densities is $div\,\epsilon_o\mathbf{E}$, which can be determined from (6).

$$\rho_u + \rho_p = \nabla \cdot \epsilon_o\mathbf{E} = -\epsilon_o\mathbf{E} \cdot \frac{\nabla\sigma}{\sigma} = -\epsilon_o\mathbf{J} \cdot \frac{\nabla\sigma}{\sigma^2} \tag{16}$$

At an abrupt discontinuity, the sum of the surface charges determines the discontinuity of normal $\mathbf{E}$. In view of (9),

$$\sigma_{su} + \sigma_{sp} = \mathbf{n} \cdot (\epsilon_o\mathbf{E}^a - \epsilon_o\mathbf{E}^b) = \mathbf{n} \cdot \epsilon_o\mathbf{E}^a\big(1 - \frac{\sigma_a}{\sigma_b}\big) \tag{17}$$

Note that the distribution of ϵ plays no part in shaping the $\mathbf{E}$ lines.

In following a typical current tube from high potential to low in the uniform conductor of Fig. 7.2.3a, no conductivity gradients are encountered, so (16) tells us there is no source of $\mathbf{E}$. Thus, it is no surprise that Φ satisfies Laplace's equation throughout the uniform conductor.

In following the current tube through the discontinuity of Fig. 7.2.3b, from low to high conductivity, (17) shows that there is a negative surface source of $\mathbf{E}$. Thus, $\mathbf{E}$ tends to be excluded from the more conducting region and intensified in the less conducting region.

With the conductivity increasing smoothly in the direction of $\mathbf{E}$, as illustrated in Fig. 7.2.3c, $\mathbf{E} \cdot \nabla\sigma$ is positive. Thus, the source of $\mathbf{E}$ is negative and the $\mathbf{E}$ lines attenuate along the flux tube.

Uniform and piece-wise uniform conductors are commonly encountered, and examples in this category are taken up in Secs. 7.4 and 7.5. Examples where the conductivity is smoothly distributed are analogous to the smoothly varying permittivity configurations exemplified in Sec. 6.7. In a simple one-dimensional configuration, the following example illustrates all three categories.

Example 7.2.1. One-Dimensional Resistors

The resistor shown in Fig. 7.2.4 has a uniform cross-section of area A in any $x - z$ plane. Over its length d it has a conductivity $\sigma(y)$. Perfectly conducting electrodes constrain the potential to be v at $y = 0$ and to be zero at $y = d$. The cylindrical conductor is surrounded by a perfect insulator.

The potential is assumed to depend only on y. Thus, the electric field and current density are y directed, and the condition that there be no component of $\mathbf{E}$ normal to the insulating boundaries is automatically satisfied. For the one-dimensional field, (4) reduces to

$$\frac{d}{dy}\big(\sigma\frac{d\Phi}{dy}\big) = 0 \tag{18}$$

The quantity in parentheses, the negative of the current density, is conserved over the length of the resistor. Thus, with J_o defined as constant,

$$\sigma\frac{d\Phi}{dy} = -J_o \tag{19}$$

This expression is now integrated from the lower electrode to an arbitrary location y.

$$\int_v^\Phi d\Phi = -\int_0^y \frac{J_o}{\sigma}dy \Rightarrow \Phi = v - \int_0^y \frac{J_o}{\sigma}dy \tag{20}$$

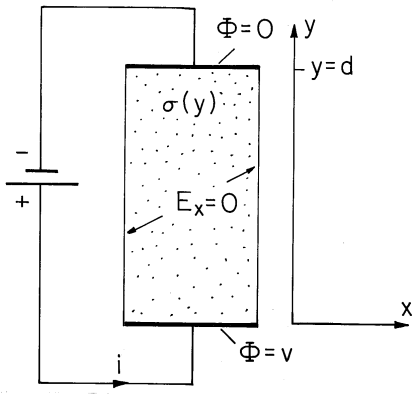

Fig. 7.2.4 Cylindrical resistor having conductivity that is a function of position y between the electrodes. The material surrounding the conductor is insulating.

Evaluation of this expression where $y = d$ and $\Phi = 0$ relates the current density to the terminal voltage.

$$v = \int_0^d \frac{J_o}{\sigma} dy \Rightarrow J_o = v / \int_0^d \frac{dy}{\sigma} \tag{21}$$

Introduction of this expression into (20) then gives the potential distribution.

$$\Phi = v\left[1 - \int_0^y \frac{dy}{\sigma} / \int_0^d \frac{dy}{\sigma}\right] \tag{22}$$

The conductance, defined by (15), follows from (21).

$$G = \frac{AJ_o}{v} = A / \int_0^d \frac{dy}{\sigma} \tag{23}$$

These relations hold for any one-dimensional distribution of σ. Of course, there is no dependence on ϵ, which could have any distribution. The permittivity could even depend on x and z. In terms of the circuit analogy suggested in the introduction, the resistors determine the distribution of voltages regardless of the interconnected capacitors.

Three special cases conform to the three categories of configurations illustrated in Fig. 7.2.3.

Uniform Conductivity. If σ is uniform, evaluation of (22) and (23) gives

$$\Phi = v\left(1 - \frac{y}{d}\right) \tag{24}$$

$$G = \frac{A\sigma}{d} \tag{25}$$

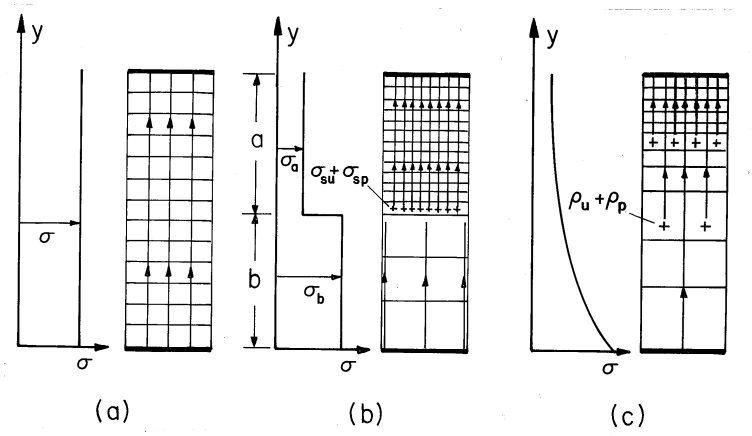

Fig. 7.2.5 Conductivity, potential, charge density, and field distributions in special cases for the configuration of Fig. 7.2.4. (a) Uniform conductivity. (b) Layers of uniform but different conductivities. (c) Exponentially varying conductivity.

The potential and electric field are the same as they would be between plane parallel electrodes in free space in a uniform perfect dielectric. However, because of the insulating walls, the conduction field remains uniform regardless of the length of the resistor compared to its transverse dimensions.

It is clear from (16) that there is no volume charge density, and this is consistent with the uniform field that has been found. These distributions of σ, Φ, and $\mathbf{E}$ are shown in Fig. 7.2.5a.

Piece-Wise Uniform Conductivity. With the resistor composed of uniformly conducting layers in series, as shown in Fig. 7.2.5b, the potential and conductance follow from (22) and (23) as

$$\Phi = \begin{cases} v\left\{1 - \frac{G}{A}\frac{y}{\sigma_b}\right\} & 0 < y < b \\ v\left\{1 - \frac{G}{A}[(b/\sigma_b) + (y-b)/\sigma_a]\right\} & b < y < a+b \end{cases} \tag{26}$$

$$G = \frac{A}{[(b/\sigma_b) + (a/\sigma_a)]} \tag{27}$$

Again, there are no sources to distort the electric field in the uniformly conducting regions. However, at the discontinuity in conductivity, (17) shows that there is surface charge. For $\sigma_b > \sigma_a$, this surface charge is positive, tending to account for the more intense field shown in Fig. 7.2.5b in the upper region.

Smoothly Varying Conductivity. With the exponential variation $\sigma = \sigma_o \exp(-y/d)$, (22) and (23) become

$$\Phi = v\left[1 - \frac{(e^{y/d} - 1)}{(e-1)}\right] \tag{28}$$

$$G = \frac{A\sigma_o}{d(e-1)} \tag{29}$$

Here the charge density that accounts for the distribution of $\mathbf{E}$ follows from (16).

$$\rho_u + \rho_p = \frac{\epsilon_o J_o}{\sigma_o d} e^{y/d} \tag{30}$$

Thus, the field is shielded from the lower region by an exponentially increasing volume charge density.

7.3 DISTRIBUTED CURRENT SOURCES AND ASSOCIATED FIELDS

Under steady conditions, conservation of charge requires that the current density be solenoidal. Thus, $\mathbf{J}$ lines do not originate or terminate. We have so far thought of current tubes as originating outside the region of interest, on the boundaries. It is sometimes convenient to introduce a volume distribution of current sources, $s(\mathbf{r}, t)$ A/m^3, defined so that the steady charge conservation equation becomes

$$\boxed{\oint_S \mathbf{J} \cdot d\mathbf{a} = \int_V s dv \Leftrightarrow \nabla \cdot \mathbf{J} = s} \tag{1}$$

The motivation for introducing a distributed source of current becomes clear as we now define singular sources and think about how these can be realized physically.

Distributed Current Source Singularities. The analogy between (1) and Gauss' law begs for the definition of point, line, and surface current sources, as depicted in Fig. 7.3.1. In returning to Sec. 1.3 where the analogous singular charge distributions were defined, it should be kept in mind that we are now considering a source of current density, not of electric flux.

A point source of current gives rise to a net current i_p out of a volume V that shrinks to zero while always enveloping the source.

$$\oint_S \mathbf{J} \cdot d\mathbf{a} = i_p \qquad i_p \equiv \lim_{\substack{s \to \infty \\ V \to 0}} \int_V s dv \tag{2}$$

Such a source might be used to represent the current distribution around a small electrode introduced into a conducting material. As shown in Fig. 7.3.1d, the electrode is connected to a source of current i_p through an insulated wire. At least under steady conditions, the wire and its insulation can be made fine enough so that the current distribution in the surrounding conductor is not disturbed.

Note that if the wire and its insulation are considered, the current density remains solenoidal. A surface surrounding the spherical electrode is pierced by the

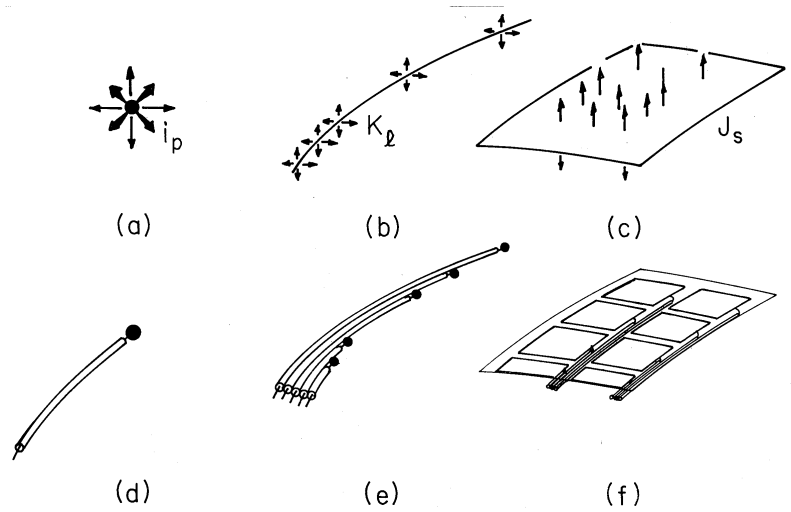

Fig. 7.3.1 Singular current source distributions represented conceptually by the top row, suggesting how these might be realized physically by the bottom row by electrodes fed through insulated wires.

wire. The contribution to the integral of $\mathbf{J}\cdot d\mathbf{a}$ from this part of the surface integral is equal and opposite to that of the remainder of the surface surrounding the electrode. The point source is, in this case, an artifice for ignoring the effect of the insulated wire on the current distribution.

The tubular volume having a cross-sectional area A used to define a line charge density in Sec. 1.3 (Fig. 1.3.4) is equally applicable here to defining a line current density.

$$K_l \equiv \lim_{\substack{s\to\infty \\ A\to 0}} \int_A s\,da \tag{3}$$

In general, K_l is a function of position along the line, as shown in Fig. 7.3.1b. If this is the case, a physical realization would require a bundle of insulated wires, each terminated in an electrode segment delivering its current to the surrounding medium, as shown in Fig. 7.3.1e. Most often, the line source is used with two-dimensional flows and describes a uniform wire electrode driven at one end by a current source.

The surface current source of Figs. 7.3.1c and 7.3.1f is defined using the same incremental control volume enclosing the surface source as shown in Fig. 1.3.5.

$$\boxed{J_s \equiv \lim_{\substack{s\to\infty \\ h\to 0}} \int_{\xi-\frac{h}{2}}^{\xi+\frac{h}{2}} s\,d\xi} \tag{4}$$

Note that J_s is the *net* current density entering the surrounding material at a given location.

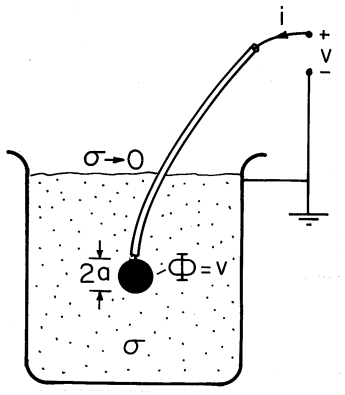

Fig. 7.3.2 For a small spherical electrode, the conductance relative to a large conductor at "infinity" is given by (7).

Fields Associated with Current Source Singularities. In the immediate vicinity of a point current source immersed in a uniform conductor, the current distribution is spherically symmetric. Thus, with $\mathbf{J} = \sigma\mathbf{E}$, the integral current continuity law, (1), requires that

$$4\pi r^2 \sigma E_r = i_p \tag{5}$$

From this, the electric field intensity and potential of a point source follow as

$$E_r = \frac{i_p}{4\pi\sigma r^2} \Rightarrow \Phi = \frac{i_p}{4\pi\sigma r} \tag{6}$$

Example 7.3.1. Conductance of an Isolated Spherical Electrode

A simple way to measure the conductivity of a liquid is based on using a small spherical electrode of radius a, as shown in Fig. 7.3.2. The electrode, connected to an insulated wire, is immersed in the liquid of uniform conductivity σ. The liquid is in a container with a second electrode having a large area compared to that of the sphere, and located many radii a from the sphere. Thus, the potential drop associated with a current i that passes from the spherical electrode to the large electrode is largely in the vicinity of the sphere.

By definition the potential at the surface of the sphere is v, so evaluation of the potential for a point source, (6), at $r = a$ gives

$$v = \frac{i}{4\pi\sigma a} \Rightarrow G \equiv \frac{i}{v} = 4\pi\sigma a \tag{7}$$

This conductance is analogous to the capacitance of an isolated spherical electrode, as given by (4.6.8). Here, a fine insulated wire connected to the sphere would have little effect on the current distribution.

The conductance associated with a contact on a conducting material is often approximated by picturing the contact as a hemispherical electrode, as shown in Fig. 7.3.3. The region above the surface is an insulator. Thus, there is no current density and hence no electric field intensity normal to this surface. Note that this condition

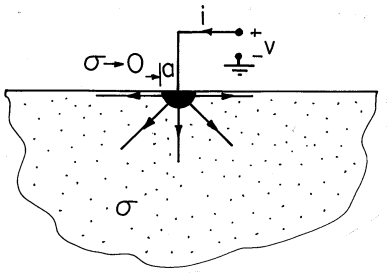

Fig. 7.3.3 Hemispherical electrode provides contact with infinite half-space of material with conductance given by (8).

is satisfied by the field associated with a point source positioned on the conductor-insulator interface. An additional requirement is that the potential on the surface of the electrode be v. Because current is carried by only half of the spherical surface, it follows from reevaluation of (6a) that the conductance of the hemispherical surface contact is

$$G = 2\pi\sigma a \tag{8}$$

The fields associated with uniform line and surface sources are analogous to those discussed for line and surface charges in Sec. 1.3.

The superposition principle, as discussed for Poisson's equation in Sec. 4.3, is equally applicable here. Thus, the fields associated with higher-order source singularities can again be found by superimposing those of the basic singular sources already defined. Because it can be used to model a battery imbedded in a conductor, the dipole source is of particular importance.

Example 7.3.2. Dipole Current Source in Spherical Coordinates

A positive point current source of magnitude i_p is located at $z = d$, just above a negative source (a sink) of equal magnitude at the origin. The source-sink pair, shown in Fig. 7.3.4, gives rise to fields analogous to those of Fig. 4.4.2. In the limit where the spacing d goes to zero while the product of the source strength and this spacing remains finite, this pair of sources forms a dipole. Starting with the potential as given for a source at the origin by (6), the limiting process is the same as leading to (4.4.8). The charge dipole moment qd is replaced by the current dipole moment $i_p d$ and $\epsilon_o \to \sigma$, $qd \to i_p d$. Thus, the potential of the dipole current source is

$$\Phi = \frac{i_p d}{4\pi\sigma}\frac{\cos\theta}{r^2} \tag{9}$$

The potential of a polar dipole current source is found in Prob. 7.3.3.

Method of Images. With the new boundary conditions describing steady current distributions come additional opportunities to exploit symmetry, as discussed in Sec. 4.7. Figure 7.3.5 shows a pair of equal magnitude point current sources located at equal distances to the right and left of a planar surface. By contrast with the point charges of Fig. 4.7.1, these sources are of the same sign. Thus,

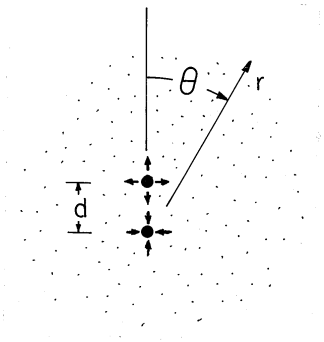

Fig. 7.3.4 Three-dimensional dipole current source has potential given by (9).

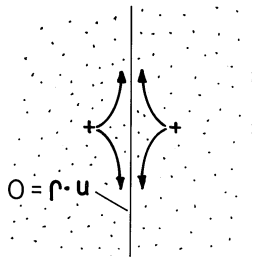

Fig. 7.3.5 Point current source and its image representing an insulating boundary.

the electric field normal to the surface is zero rather than the tangential field. The field and current distribution in the right half is the same as if that region were filled by a uniform conductor and bounded by an insulator on its left.

7.4 SUPERPOSITION AND UNIQUENESS OF STEADY CONDUCTION SOLUTIONS

The physical laws and boundary conditions are different, but the approach in this section is similar to that of Secs. 5.1 and 5.2 treating Poisson's equation.

In a material having the conductivity distribution $\sigma(\mathbf{r})$ and source distribution $s(\mathbf{r})$, a steady potential distribution Φ must satisfy (7.2.4) with a source density $-s$ on the right. Typically, the configurations of interest are as in Fig. 7.2.1, except that we now include the possibility of a distribution of current source density in the volume V. Electrodes are used to constrain this potential over some of the surface enclosing the volume V occupied by this material. This part of the surface, where the material contacts the electrodes, will be called S'. We will assume here that on the remainder of the enclosing surface, denoted by S'', the normal current density is specified. Depicted in Fig. 7.2.1 is the special case where the boundary S'' is insulating and hence where the normal current density is zero. Thus, according to

(7.2.1), (7.2.3), and (7.3.1), the desired $\mathbf{E}$ and $\mathbf{J}$ are found from a solution Φ to

$$\nabla \cdot \sigma \nabla \Phi = -s \tag{1}$$

where

$$\Phi = \Phi_i \quad \text{on} \quad S_i'$$

$$-\mathbf{n} \cdot \sigma \nabla \Phi = J_i \quad \text{on} \quad S_i''$$

Except for the possibility that part of the boundary is a surface S'' where the normal current density rather than the potential is specified, the situation here is analogous to that in Sec. 5.1. The solution can be divided into a particular part [that satisfies the differential equation of (1) at each point in the volume, but not the boundary conditions] and a homogeneous part. The latter is then adjusted to make the sum of the two satisfy the boundary conditions.

Superposition to Satisfy Boundary Conditions. Suppose that a system is composed of a source-free conductor ($s = 0$) contacted by one reference electrode at ground potential and n electrodes, respectively, at the potentials v_j, $j = 1, \ldots n$. The contacting surfaces of these electrodes comprise the surface S'. As shown in Fig. 7.2.1, there may be other parts of the surface enclosing the material that are insulating ($J_i = 0$) and denoted by S''. The solution can be represented as the sum of the potential distributions associated with each of the electrodes of specified potential while the others are grounded.

$$\Phi = \sum_{j=1}^{n} \Phi_j \tag{2}$$

where

$$\nabla \cdot \sigma \nabla \Phi_j = 0$$

$$\Phi_j = \begin{cases} v_j & \text{on } S_i', \quad j = i \\ 0 & \text{on } S_i', \quad j \neq i \end{cases}$$

Each Φ_j satisfies (1) with $s = 0$ and the boundary condition on S_i'' with $J_i = 0$. This decomposition of the solution is familiar from Sec. 5.1. However, the boundary condition on the insulating surface S'' requires a somewhat broadened view of what is meant by the respective terms in (2). As the following example illustrates, modes that have zero derivatives rather than zero amplitude at boundaries are now useful for satisfying the insulating boundary condition.

Example 7.4.1. Modal Solution with an Insulating Boundary

In the two-dimensional configuration of Fig. 7.4.1, a uniformly conducting material is grounded along its left edge, bounded by insulating material along its right edge,

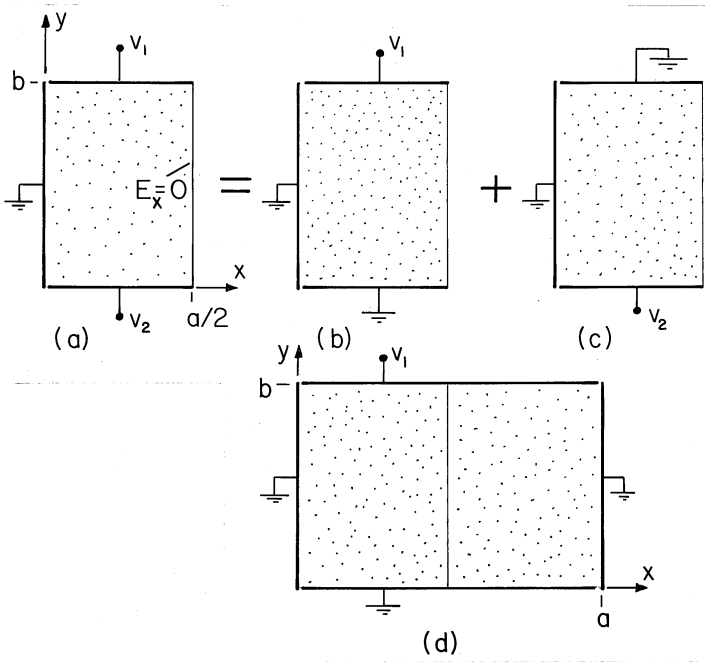

Fig. 7.4.1 (a) Two terminal pairs attached to conducting material having one wall at zero potential and another that is insulating. (b) Field solution is broken into part due to potential v_1 and (c) potential v_2. (d) The boundary condition at the insulating wall is satisfied by using the symmetry of an equivalent problem with all of the walls constrained in potential.

and driven by electrodes having the potentials v_1 and v_2 at the top and bottom, respectively.

Decomposition of the potential, as called for by (2), amounts to the superposition of the potentials for the two problems of (b) and (c) in the figure. Note that for each of these, the normal derivative of the potential must be zero at the right boundary.

Pictured in part (d) of Fig. 7.4.1 is a configuration familiar from Sec. 5.5. The potential distribution for the configuration of Fig. 5.5.2, (5.5.9), is equally applicable to that of Fig. 7.4.1. This is so because the symmetry requires that there be no x-directed electric field along the surface $x = a/2$. In turn, the potential distribution for part (c) is readily determined from this one by replacing $v_1 \rightarrow v_2$ and $y \rightarrow b - y$. Thus, the total potential is

$$\Phi = \sum_{\substack{n=1 \\ \text{odd}}}^{\infty} \frac{4}{\pi} \left\{ \frac{v_1}{n} \frac{\sinh\left(\frac{n\pi}{a}y\right)}{\sinh\left(\frac{n\pi}{a}b\right)} \sin\frac{n\pi}{a}x + \frac{v_2}{n} \frac{\sinh\left[\frac{n\pi}{a}(b-y)\right]}{\sinh\left(\frac{n\pi b}{a}\right)} \sin\frac{n\pi}{a}x \right\} \tag{3}$$

If we were to solve this problem without reference to Sec. 5.5, the modes used to expand the electrode potential would be zero at $x = 0$ and have zero derivative at the insulating boundary (at $x = a/2$).

The Conductance Matrix. With S_i' defined as the surface over which the i-th electrode contacts the conducting material, the current emerging from that electrode is

$$i_i = \int_{S_i} \sigma \nabla \Phi \cdot d\mathbf{a} \tag{4}$$

[See Fig. 7.2.1 for definition of direction of $d\mathbf{a}$.] In terms of the potential decomposition represented by (2), this expression becomes

$$i_i = \sum_{j=1}^{n} \int_{S_i'} \sigma \nabla \Phi_j \cdot d\mathbf{a} = \sum_{j=1}^{n} G_{ij} v_j \tag{5}$$

where the conductances are

$$\boxed{G_{ij} = \frac{\int_{S_i'} \sigma \nabla \Phi_j \cdot d\mathbf{a}}{v_j}} \tag{6}$$

Because Φ_j is by definition proportional to v_j, these parameters are independent of the excitations. They depend only on the physical properties and geometry of the configuration.

Example 7.4.2. Two Terminal Pair Conductance Matrix

For the system of Fig. 7.4.1, (5) becomes

$$\begin{bmatrix} i_1 \\ i_2 \end{bmatrix} = \begin{bmatrix} G_{11} & G_{12} \\ G_{21} & G_{22} \end{bmatrix} \begin{bmatrix} v_1 \\ v_2 \end{bmatrix} \tag{7}$$

With the potential given by (3), the *self-conductances* G_{11} and G_{22} and the *mutual conductances* G_{12} and G_{21} follow by evaluation of (5). This potential is singular in the left-hand corners, so the self-conductances determined in this way are represented by a series that does not converge. However, the mutual conductances are determined by integrating the current density over an electrode that is at the same potential as the grounded wall, so they are well represented. For example, with c defined as the length of the conducting block in the z direction,

$$G_{12} = \frac{\sigma c}{v_2} \int_0^{a/2} \frac{\partial \Phi_2}{\partial y}\Big|_{y=b} dx = \frac{4}{\pi} \sigma c \sum_{\substack{n=1 \\ \text{odd}}}^{\infty} \frac{1}{n \sinh\left(\frac{n\pi b}{a}\right)} \tag{8}$$

Uniqueness. With Φ_i, J_i, $\sigma(\mathbf{r})$, and $s(\mathbf{r})$ given, a steady current distribution is uniquely specified by the differential equation and boundary conditions of (1). As in Sec. 5.2, a proof that a second solution must be the same as the first hinges on defining a difference potential $\Phi_d = \Phi_a - \Phi_b$ and showing that, because $\Phi_d = 0$ on S_i' and $\mathbf{n} \cdot \sigma \nabla \Phi_d = 0$ on S_i'' in Fig. 7.2.1, Φ_d must be zero.

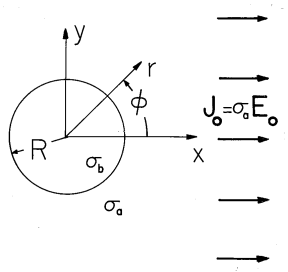

Fig. 7.5.1 Conducting circular rod is immersed in a conducting material supporting a current density that would be uniform in the absence of the rod.

7.5 STEADY CURRENTS IN PIECE-WISE UNIFORM CONDUCTORS

Conductor configurations are often made up from materials that are uniformly conducting. The conductivity is then uniform in the subregions occupied by the different materials but undergoes step discontinuities at interfaces between regions. In the uniformly conducting regions, the potential obeys Laplace's equation, (7.2.5),

$$\nabla^2\Phi = 0 \tag{1}$$

while at the interfaces between regions, the continuity conditions require that the normal current density and tangential electric field intensity be continuous, (7.2.9) and (7.2.10).

$$\mathbf{n}\cdot(\sigma_a\mathbf{E}^a - \sigma_b\mathbf{E}^b) = 0 \tag{2}$$

$$\Phi^a - \Phi^b = 0 \tag{3}$$

Analogy to Fields in Linear Dielectrics. If the conductivity is replaced by the permittivity, these laws are identical to those underlying the examples of Sec. 6.6. The role played by $\mathbf{D}$ is now taken by $\mathbf{J}$. Thus, the analysis for the following example has already been carried out in Sec. 6.6.

Example 7.5.1. Conducting Circular Rod in Uniform Transverse Field

A rod of radius R and conductivity σ_b is immersed in a material of conductivity σ_a, as shown in Fig. 7.5.1. Perhaps imposed by means of plane parallel electrodes far to the right and left, there is a uniform current density far from the cylinder.

The potential distribution is deduced using the same steps as in Example 6.6.2, with $\epsilon_a \to \sigma_a$ and $\epsilon_b \to \sigma_b$. Thus, it follows from (6.6.21) and (6.6.22) as

$$\Phi_a = -RE_o\cos\phi\left[\left(\frac{r}{R}\right) - \left(\frac{R}{r}\right)\frac{(\sigma_b-\sigma_a)}{(\sigma_b+\sigma_a)}\right] \tag{4}$$

$$\Phi_b = \frac{-2\sigma_a}{\sigma_a+\sigma_b}E_o r\cos\phi \tag{5}$$

and the lines of *electric field intensity* are as shown in Fig. 6.6.6. Note that although the lines of $\mathbf{E}$ and $\mathbf{J}$ are in the same direction and have the same pattern in each of the

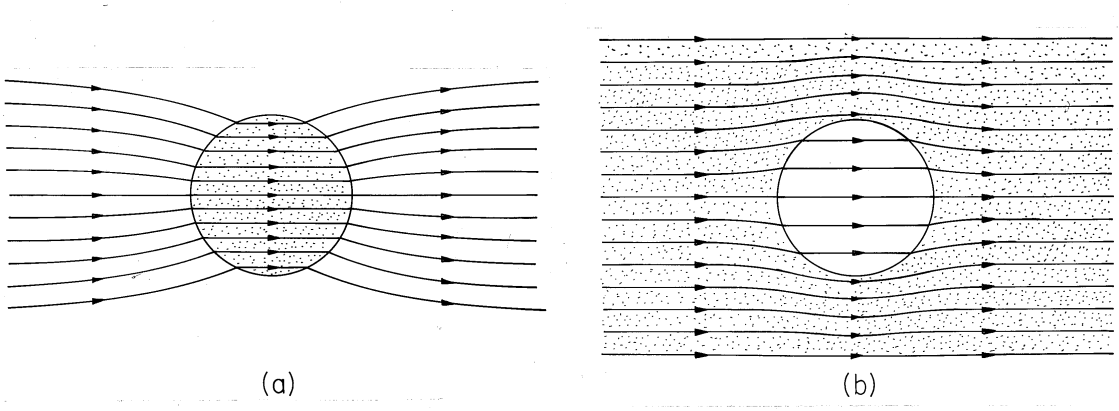

Fig. 7.5.2 Distribution of current density in and around the rod of Fig. 7.5.1. (a) $\sigma_b \geq \sigma_a$. (b) $\sigma_a \geq \sigma_b$.

regions, they have very different behaviors where the conductivity is discontinuous. In fact, the normal component of the current density is continuous at the interface, and the spacing between lines of **J** must be preserved across the interface. Thus, in the distribution of *current density* shown in Fig. 7.5.2, the lines are continuous. Note that the current tends to concentrate on the rod if it is more conducting, but is diverted around the rod if it is more insulating.

A surface charge density resides at the interface between the conducting media of different conductivities. This surface charge density acts as the source of **E** on the cylindrical surface and is identified by (7.2.17).

Inside-Outside Approximations. In exploiting the formal analogy between fields in linear dielectrics and in Ohmic conductors, it is important to keep in mind the very different physical phenomena being described. For example, there is no conduction analog to the free space permittivity ϵ_o. There is no minimum value of the conductivity, and although ϵ can vary between a minimum of ϵ_o in free space and $1000\epsilon_o$ or more in special solids, the electrical conductivity is even more widely varying. The ratio of the conductivity of a copper wire to that of its insulation exceeds 10^{21}.

Because some materials are very good conductors while others are very good insulators, steady conduction problems can exemplify the determination of fields for large ratios of physical parameters. In Sec. 6.6, we examined field distributions in cases where the ratios of permittivities were very large or very small. The "inside-outside" viewpoint is applicable not only to approximating fields in dielectrics but to finding the fields in the transient EQS systems in the latter part of this chapter and in MQS systems with magnetization and conduction.

Before attempting a more general approach, consider the following example, where the fields in and around a resistor are described.

Example 7.5.2. Fields in and around a Conductor

The circular cylindrical conductor of Fig. 7.5.3, having radius b and length L, is surrounded by a perfectly conducting circular cylindrical "can" having inside

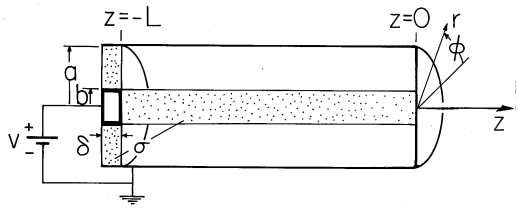

Fig. 7.5.3 Circular cylindrical conductor surrounded by coaxial perfectly conducting "can" that is connected to the right end by a perfectly conducting "short" in the plane $z = 0$. The left end is at potential v relative to right end and surrounding wall and is connected to that wall at $z = -L$ by a washer-shaped resistive material.

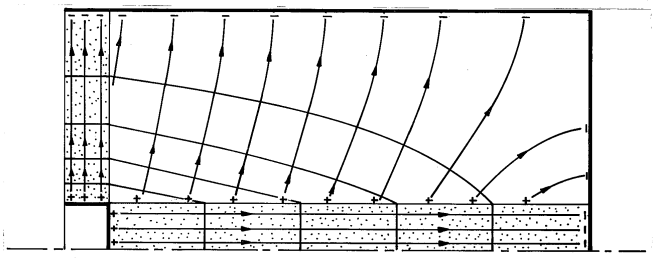

Fig. 7.5.4 Distribution of potential and electric field intensity for the configuration of Fig. 7.5.3.

radius a. With respect to the surrounding perfectly conducting shield, a dc voltage source applies a voltage v to the perfectly conducting disk. A washer-shaped material of thickness δ and also having conductivity σ is connected between the perfectly conducting disk and the outer can. What are the distributions of Φ and $\mathbf{E}$ in the conductors and in the annular free space region?

Note that the fields within each of the conductors are fully specified without regard for the shape of the can. The surfaces of the circular cylindrical conductor are either constrained in potential or bounded by free space. On the latter, the normal component of $\mathbf{J}$, and hence of $\mathbf{E}$, is zero. Thus, in the language of Sec. 7.4, the potential is constrained on S' while the normal derivative of Φ is constrained on the insulating surfaces S''. For the center conductor, S' is at $z = 0$ and $z = -L$ while S'' is at $r = b$. For the washer-shaped conductor, S' is at $r = b$ and $r = a$ and S'' is at $z = -L$ and $z = -(L + \delta)$. The theorem of Sec. 7.4 shows that the potential inside each of the conductors is uniquely specified. Note that this is true regardless of the arrangement outside the conductors.

In the cylindrical conductor, the solution for the potential that satisfies Laplace's equation and all these boundary conditions is simply a linear function of z.

$$\Phi^b = -\frac{v}{L}z \tag{6}$$

Thus, the electric field intensity is uniform and z directed.

$$\mathbf{E}^b = \frac{v}{L}\mathbf{i_z} \tag{7}$$

These equipotentials and $\mathbf{E}$ lines are sketched in Fig. 7.5.4. By way of reinforcing what is new about the insulating surface boundary condition, note that (6) and (7) apply to the cylindrical conductor regardless of its cross-section geometry and its length. However, the longer it is, the more stringent is the requirement that the annular region be insulating compared to the central region.

In the washer-shaped conductor, the axial symmetry requires that the potential not depend on z. If it depends only on the radius, the boundary conditions on the insulating surfaces are automatically satsfied. Two solutions to Laplace's equation are required to meet the potential constraints at $r = a$ and $r = b$. Thus, the solution is assumed to be of the form

$$\Phi^c = Alnr + B \tag{8}$$

The coefficients A and B are determined from the radial boundary conditions, and it follows that the potential within the washer-shaped conductor is

$$\Phi^c = v\frac{ln\left(\frac{r}{a}\right)}{ln\left(\frac{b}{a}\right)} \tag{9}$$

The "inside" fields can now be used to determine those in the insulating annular "outside" region. The potential is determined on all of the surface surrounding this region. In addition to being zero on the surfaces $r = a$ and $z = 0$, the potential is given by (6) at $r = b$ and by (9) at $z = -L$. So, in turn, the potential in this annular region is uniquely determined.

This is one of the few problems in this book where solutions to Laplace's equation that have both an r and a z dependence are considered. Because there is no ϕ dependence, Laplace's equation requires that

$$\left(\frac{\partial^2}{\partial z^2} + \frac{1}{r}\frac{\partial}{\partial r}r\frac{\partial}{\partial r}\right)\Phi = 0 \tag{10}$$

The linear dependence on z of the potential at $r = b$ suggests that solutions to Laplace's equation take the product form $R(r)z$. Substitution into (10) then shows that the r dependence is the same as given by (9). With the coefficients adjusted to make the potential $\Phi_a(a, -L) = 0$ and $\Phi_a(b, -L) = v$, it follows that in the outside insulating region

$$\Phi^a = \frac{v}{ln\left(\frac{a}{b}\right)}ln\left(\frac{r}{a}\right)\frac{z}{L} \tag{11}$$

To sketch this potential and the associated **E** lines in Fig. 7.5.4, observe that the equipotentials join points of the given potential on the central conductor with those of the same potential on the washer-shaped conductor. Of course, the zero potential surface is at $r = a$ and at $z = 0$. The lines of electric field intensity that originate on the surfaces of the conductors are perpendicular to these equipotentials and have tangential components that match those of the inside fields. Thus, at the surfaces of the finite conductors, the electric field in region (a) is neither perpendicular nor tangential to the boundary.

For a positive potential v, it is clear that there must be positive surface charge on the surfaces of the conductors bounding the annular insulating region. Remember that the normal component of **E** on the conductor sides of these surfaces is zero. Thus, there is a surface charge that is proportional to the normal component of **E** on the insulating side of the surfaces.

$$\sigma_s(r = b) = \epsilon_o E_r^a(r = b) = -\frac{\epsilon_o v}{b\,ln(a/b)}\frac{z}{L} \tag{12}$$

The order in which we have determined the fields makes it clear that this surface charge is the one required to accommodate the field configuration outside

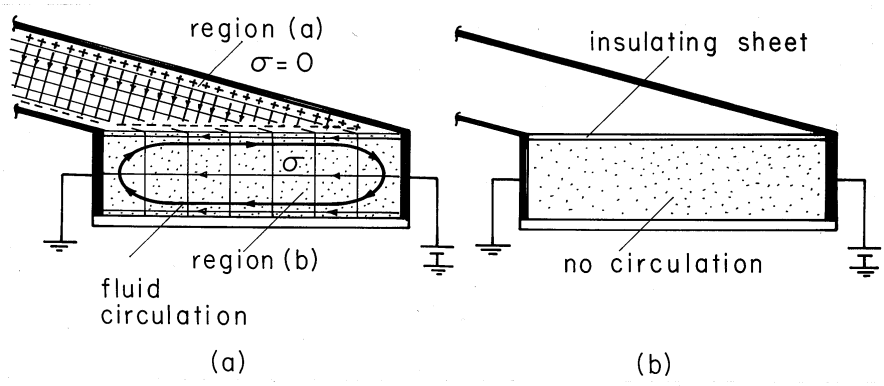

Fig. 7.5.5 Demonstration of the absence of volume charge density and existence of a surface charge density for a uniform conductor. (a) A slightly conducting oil is contained by a box constructed from a pair of electrodes to the left and right and with insulating walls on the other two sides and the bottom. The top surface of the conducting oil is free to move. The resulting surface force density sets up a circulating motion of the liquid, as shown. (b) With an insulating sheet resting on the interface, the circulating motion is absent.

the conducting regions. A change in the shield geometry changes Φ^a but does not alter the current distribution within the conductors. In terms of the circuit analogy used in Sec. 7.0, the potential distributions have been completely determined by the rod-shaped and washer-shaped resistors. The charge distribution is then determined *ex post facto* by the "distributed capacitors" surrounding the resistors.

The following demonstration shows that the unpaired charge density is zero in the volume of a uniformly conducting material and that charges do indeed tend to accumulate at discontinuities of conductivity.

Demonstration 7.5.1. Distribution of Unpaired Charge

A box is constructed so that two of its sides and its bottom are plexiglas, the top is open, and the sides shown to left and right in Fig. 7.5.5 are highly conducting. It is filled with corn oil so that the region between the vertical electrodes in Fig. 7.5.5 is semi-insulating. The region above the free surface is air and insulating compared to the corn oil. Thus, the corn oil plays a role analogous to that of the cylindrical rod in Example 7.5.2. Consistent with its insulating transverse boundaries and the potential constraints to left and right is an "inside" electric field that is uniform.

The electric field in the outside region (a) determines the distribution of charge on the interface. Since we have determined that the inside field is uniform, the potential of the interface varies linearly from v at the right electrode to zero at the left electrode. Thus, the equipotentials are evenly spaced along the interface. The equipotentials in the outside region (a) are planes joining the inside equipotentials and extending to infinity, parallel to the canted electrodes. Note that this field satisfies the boundary conditions on the slanted electrodes and matches the potential on the liquid interface. The electric field intensity is uniform, originating on the upper electrode and terminating either on the interface or on the lower slanted electrode. Because both the spacing and the potential difference vary linearly with horizontal distance, the negative surface charge induced on the interface is uniform.

Wherever there is an unpaired charge density, the corn oil is subject to an electrical force. There is unpaired charge in the immediate vicinity of the interface in the form of a surface charge, but not in the volume of the conductor. Consistent with this prediction is the observation that with the application of about 20 kV to electrodes having 20 cm spacing, the liquid is set into a circulating motion. The liquid moves rapidly to the right at the interface and recirculates in the region below. Note that the force at the interface is indeed to the right because it is proportional to the product of a negative charge and a negative electric field intensity. The fluid moves as though each part of the interface is being pulled to the right. But how can we be sure that the circulation is not due to forces on unpaired charges in the fluid volume?

An alteration to the same experiment answers this question. With a plexiglas sheet placed on the interface, it is mechanically pinned down. That is, the electrical force acting on the unpaired charges in the immediate vicinity of the interface is countered by viscous forces tending to prevent the fluid from moving tangential to the solid boundary. Yet because the sheet is insulating, the field distribution within the conductor is presumably unaltered from what it was before.

With the plexiglas sheet in place, the circulations of the first experiment are no longer observed. This is consistent with a model that represents the corn-oil as a uniform Ohmic conductor[1]. (For a mathematical analysis, see Prob. 7.5.3.)

In general, there is a two-way coupling between the fields in adjacent uniformly conducting regions. If the ratio of conductivities is either very large or very small, it is possible to calculate the fields in an "inside" region ignoring the effect of "outside" regions, and then to find the fields in the "outside" region. The region in which the field is first found, the "inside" region, is usually the one to which the excitation is applied, as illustrated in Example 7.5.2. This will be further illustrated in the following example, which pursues an approximate treatment of Example 7.5.1. The exact solutions found there can then be compared to the approximate ones.

Example 7.5.3. Approximate Current Distribution around Relatively Insulating and Conducting Rods

Consider first the field distribution around and then in a circular rod that has a small conductivity relative to its surroundings. Thus, in Fig. 7.5.1, $\sigma_a \gg \sigma_b$. Electrodes far to the left and right are used to apply a uniform field and current density to region (a). It is therefore in this inside region outside the cylinder that the fields are first approximated.

With the rod relatively insulating, it imposes on region (a) the approximate boundary condition that the normal current density, and hence the radial derivative of the potential, be zero at the rod surface, where $r = R$.

$$\mathbf{n} \cdot \mathbf{J}^a \approx 0 \Rightarrow \frac{\partial \Phi^a}{\partial r} \approx 0 \quad \text{at} \quad r = R \tag{13}$$

Given that the field at infinity must be uniform, the potential distribution in region (a) is now uniquely specified. A solution to Laplace's equation that satisfies this condition at infinity and includes an arbitrary coefficient for hopefully satisfying the

[1] See film *Electric Fields and Moving Media*, produced by the National Committee for Electrical Engineering Films and distributed by Education Development Center, 39 Chapel St., Newton, Mass. 02160.

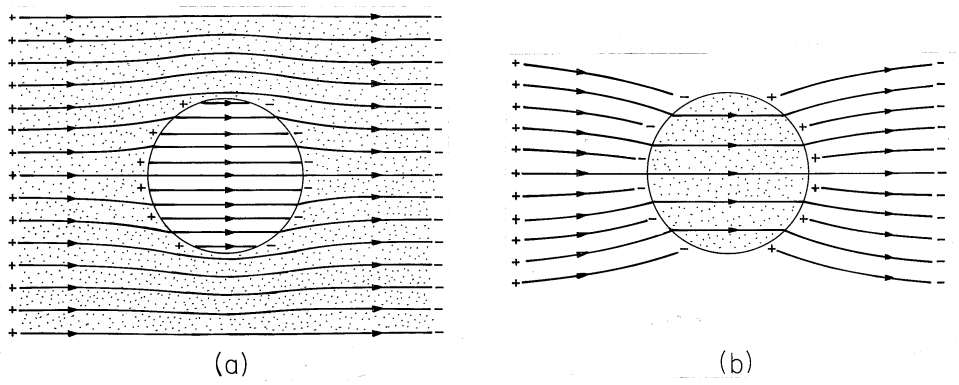

Fig. 7.5.6 Distributions of *electric field* intensity around conducting rod immersed in conducting medium: (a) $\sigma_a \gg \sigma_b$; (b) $\sigma_b \gg \sigma_a$. Compare these to distributions of *current density* shown in Fig. 7.5.2.

first condition is

$$\Phi^a = -E_o r\cos\phi + A\frac{\cos\phi}{r} \tag{14}$$

With A adjusted to satisfy (13), the approximate potential in region (a) is

$$\Phi^a = -E_o\Big(r + \frac{R^2}{r}\Big)\cos\phi \tag{15}$$

This is the potential in the exterior region, implying the field lines shown in Fig. 7.5.6a.

Now that we have obtained the approximate potential at $r = R$, $\Phi_b = -2E_oR\cos(\phi)$, we can in turn approximate the potential in region (b).

$$\Phi^b = Br\cos\phi = -2E_o r\cos\phi \tag{16}$$

The field lines associated with this potential are also shown in Fig. 7.5.6a. Note that if we take the limits of (4) and (5) where $\sigma_a/\sigma_b \gg 1$, we obtain these potentials.

Contrast these steps with those that are appropriate in the opposite extreme, where $\sigma_a/\sigma_b \ll 1$. There the rod tends to behave as an equipotential and the boundary condition at $r = R$ is $\Phi_a = \text{constant} = 0$. This condition is now used to evaluate the coefficient A in (14) to obtain

$$\Phi^a = -E_o\Big(r - \frac{R^2}{r}\Big)\cos\phi \tag{17}$$

This potential implies that there is a current density at the rod surface given by

$$J_r^a(r=R) = -\sigma_a\frac{\partial\Phi^a}{\partial r}(r=R) = 2\sigma_a E_o\cos\phi \tag{18}$$

The normal current density at the inside surface of the rod must be the same, so the coefficient B in (16) can be evaluated.

$$\Phi_b = -\frac{2\sigma_a}{\sigma_b}E_o r\cos\phi \tag{19}$$

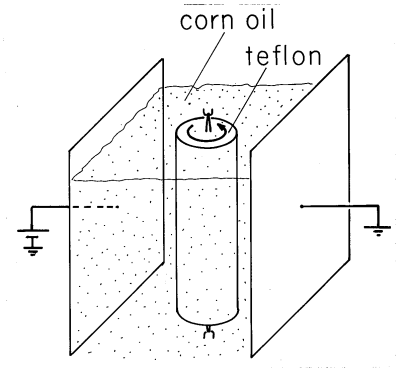

Fig. 7.5.7 Rotor of insulating material is immersed in somewhat conducting corn oil. Plane parallel electrodes are used to impose constant electric field, so from the top, the distribution of electric field should be that of Fig. 7.5.6a, at least until the rotor begins to rotate spontaneously in either direction.

Now the field lines are as shown in Fig. 7.5.6b.

Again, the approximate potential distributions given by (17) and (19), respectively, are consistent with what is obtained from the exact solutions, (4) and (5), in the limit $\sigma_a/\sigma_b \ll 1$.

In the following demonstration, a surprising electromechanical response has its origins in the charge distribution implied by the potential distributions found in Example 7.5.3.

Demonstration 7.5.2. Rotation of an Insulating Rod in a Steady Current

In the apparatus shown in Fig. 7.5.7, a teflon rod is mounted at its ends on bearings so that it is free to rotate. It, and a pair of plane parallel electrodes, are immersed in corn oil. Thus, from the top, the configuration is as shown in Fig. 7.5.1. The applied field $E_o = v/d$, where v is the voltage applied between the electrodes and d is their spacing. In the experiment, $R = 1.27$ cm , $d = 11.8$ cm, and the applied voltage is 10–20 kV.

As the voltage is raised, there is a threshold at which the rod begins to rotate. With the voltage held fixed at a level above the threshold, the ensuing rotation is continuous and in either direction. [See footnote 1.]

To explain this "motor," note that even though the corn oil used in the experiment has a conductivity of $\sigma_a = 5 \times 10^{-11}$ S/m, that is still much greater than the conductivity σ_b of the rod. Thus, the potential around and in the rod is given by (15) and (16) and the $\mathbf{E}$ field distribution is as shown in Fig. 7.5.6a. Also shown in this figure is the distribution of unpaired surface charge, which can be evaluated using (16).

$$\sigma_s(r=R) = \mathbf{n}\cdot(\epsilon_a E_r^a - \epsilon_b E_r^b) = \epsilon_b \frac{\partial \Phi^b}{\partial r}(r=R) = -2\epsilon_b E_o \cos\phi \tag{20}$$

Positive charges on the left electrode induce charges of the *same* sign on the nearer side of the rod, as do the negative charges on the electrode to the right. Thus, when static, the rod is in a posture analogous to that of a compass needle oriented

backwards in a magnetic field. Its static state is unstable and it attempts to reorient itself in the field. The continuous rotation results because once it begins to rotate, additional fields are generated that allow the charge to leak off the cylinder through currents in the surrounding oil.

Note that if the rod were much more conducting than its surroundings, charges on the electrodes would induce charges of opposite sign on the nearer surfaces of the rod. This more familiar situation is the one shown in Fig. 7.5.6b.

The condition requiring that there be no normal current density at an insulating boundary can have a dramatic effect on fringing fields. This has already been illustrated by Example 7.5.2, where the field was uniform in the central conductor no matter what its length relative to its radius. Whenever we take the resistance of a wire having length L, cross-sectional area A, and conductivity σ as being $L/\sigma A$, we exploit this boundary condition.

The conduction analogue of Example 6.6.3 gives a further illustration of how an insulating boundary ducts the electric field intensity. With $\epsilon_a \to \sigma_a$ and $\epsilon_b \to \sigma_b$, the configuration of Fig. 6.6.8 becomes the edge of a plane parallel resistor filled out to the edge of the electrodes by a material having conductivity σ_b. The fringing field then depends on the conductivity σ_a of the surrounding material.

The fringing field that would result if the entire region were filled by a material having a uniform conductivity is shown in Fig. 6.6.9a. By contrast, the field distribution with the conducting material extending only to the edge of the electrode is shown in Fig. 6.6.9b. The field inside is exactly uniform and independent of the geometry of what is outside. Of course, there is always a fringing field outside that does depend on the outside geometry. But because there is little associated current density, the resistance is unaffected by this part of the field.

7.6 CONDUCTION ANALOGS

The potential distribution for steady conduction is determined by solving (7.4.1)

$$\nabla \cdot \sigma \nabla \Phi_c = -s \tag{1}$$

in a volume V having conductivity $\sigma(\mathbf{r})$ and current source distribution $s(\mathbf{r})$, respectively.

On the other hand, if the volume is filled by a perfect dielectric having permittivity $\epsilon(\mathbf{r})$ and unpaired charge density distribution $\rho_u(\mathbf{r})$, respectively, the potential distribution is determined by the combination of (6.5.1) and (6.5.2).

$$\nabla \cdot \epsilon \nabla \Phi_e = -\rho_u \tag{2}$$

It is clear that solutions pertaining to one of these physical situations are solutions for the other, provided that the boundary conditions are also analogous. We have been exploiting this analogy in Sec. 7.5 for piece-wise continuous systems. There, solutions for the fields in dielectrics were applied to conduction problems. Of course, measurements made on dielectrics can also be used to predict steady conduction phemonena.

Conversely, fields found either theoretically or by experimentation in a steady conduction situation can be used to describe those in perfect dielectrics. When measurements are used, the latter procedure is a particularly useful one, because conduction processes are conveniently simulated and comparatively easy to measure. It is more difficult to measure the potential in free space than in a conductor, and to measure a capacitance than a resistance.

Formally, a quantitative analogy is established by introducing the constant ratios for the magnitudes of the properties, sources, and potentials, respectively, in the two systems throughout the volumes and on the boundaries. With k_1 and k_2 defined as scaling constants,

$$\frac{\epsilon}{\sigma} = k_1, \qquad \frac{\Phi_c}{\Phi_e} = k_2, \qquad \frac{k_2}{k_1} = \frac{s}{\rho_u} \tag{3}$$

substitution of the conduction variables into (2) converts it into (1). The boundary conditions on surfaces S' where the potential is constrained are analogous, provided the boundary potentials also have the constant ratio k_2 given by (3).

Most often, interest is in systems where there are no volume source distributions. Thus, suppose that the capacitance of a pair of electrodes is to be determined by measuring the conductance of analogously shaped electrodes immersed in a conducting material. The ratio of the measured capacitance to conductance, the ratio of (6.5.6) to (7.2.15), follows from substituting $\epsilon = k_1\sigma$, (3a),

$$\frac{C}{G} = \frac{\int_{S_1} \epsilon \mathbf{E} \cdot d\mathbf{a}/v}{\int_{S_1} \sigma \mathbf{E} \cdot d\mathbf{a}/v} = \frac{k_1 \int_{S_1} \sigma \mathbf{E} \cdot d\mathbf{a}/v}{\int_{S_1} \sigma \mathbf{E} \cdot d\mathbf{a}/v} = k_1 = \frac{\epsilon}{\sigma} \tag{4}$$

In multiple terminal pair systems, the capacitance matrix defined by (5.1.12) and (5.1.13) is similarly deduced from measurement of a conductance matrix, defined in (7.4.6).

Demonstration 7.6.1. Electrolyte-Tank Measurements

If great accuracy is required, fields in complex geometries are most easily determined numerically. However, especially if the capacitance is sought– and not a detailed field mapping– a conduction analog can prove convenient. A simple experiment to determine the capacitance of a pair of electrodes is shown in Fig. 7.6.1, where they are mounted on insulated rods, contacted through insulated wires, and immersed in tap water. To avoid electrolysis, where the conductors contact the water, low-frequency ac is used. Care should be taken to insure that boundary conditions imposed by the tank wall are either analogous or inconsequential.

Often, to motivate or justify approximations used in analytical modeling of complex systems, it is helpful to probe the potential distribution using such an experiment. The probe consists of a small metal tip, mounted and wired like the electrodes, but connected to a divider. By setting the probe potential to the desired rms value, it is possible to trace out equipotential surfaces by moving the probe in such a way as to keep the probe current nulled. Commercial equipment is automated with a feedback system to perform such measurements with great precision. However, given the alternative of numerical simulation, it is more likely that such approaches are appropriate in establishing rough approximations.

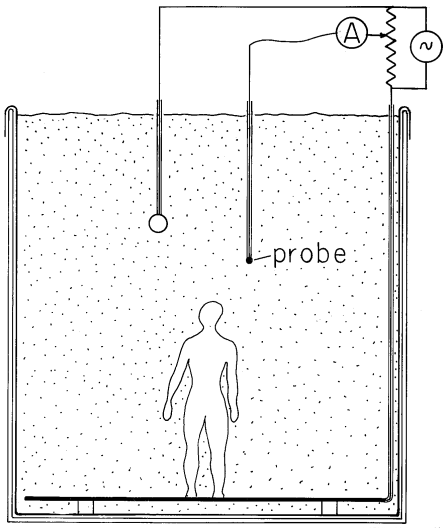

Fig. 7.6.1 Electrolytic conduction analog tank for determining potential distributions in complex configurations.

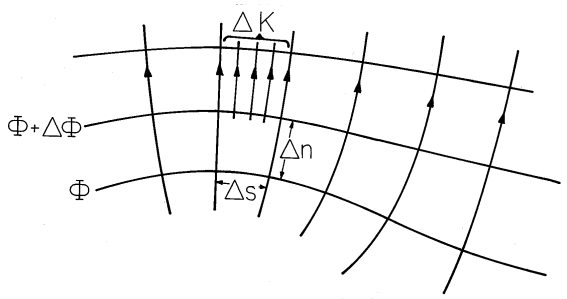

Fig. 7.6.2 In two dimensions, equipotential and field lines predicted by Laplace's equation form a grid of curvilinear squares.

Mapping Fields that Satisfy Laplace's Equation. Laplace's equation determines the potential distribution in a volume filled with a material of uniform conductivity that is source free. Especially for two-dimensional fields, the conduction analog then also gives the opportunity to refine the art of sketching the equipotentials of solutions to Laplace's equation and the associated field lines.

Before considering how a sheet of conducting paper provides the medium for determining two-dimensional fields, it is worthwhile to identify the properties of a field sketch that indeed represents a two-dimensional solution to Laplace's equation.

A review of the many two-dimensional plots of equipotentials and fields given in Chaps. 4 and 5 shows that they form a grid of curvilinear rectangles. In terms of variables defined for the field sketch of Fig. 7.6.2, where the distance between equipotentials is denoted by Δn and the distance between $\mathbf{E}$ lines is Δs, the ratio $\Delta n/\Delta s$ tends to be constant, as we shall now show.

The condition that the field be irrotational gives

$$\mathbf{E} = -\nabla\Phi \Rightarrow |\mathbf{E}| \approx \frac{|\Delta\Phi|}{|\Delta n|} \tag{5}$$

while the steady charge conservation law implies that along a flux tube,

$$\nabla \cdot \sigma\mathbf{E} = 0 \Rightarrow \sigma|\mathbf{E}|\Delta s = \text{constant} \equiv \Delta K \tag{6}$$

Thus, along a flux tube,

$$\sigma\frac{\Delta\Phi}{\Delta n}\Delta s = \Delta K \Rightarrow \frac{\Delta s}{\Delta n} = \frac{\Delta K}{\sigma\Delta\Phi} = \text{constant} \tag{7}$$

If each of the flux tubes carries the same current, and if the equipotential lines are drawn for equal increments of $\Delta\Phi$, then the ratio $\Delta s/\Delta n$ must be constant throughout the mapping. The sides of the curvilinear rectangles are commonly made equal, so that the equipotentials and field lines form a grid of curvilinear squares.

The faithfulness to Laplace's equation of a map of equipotentials at equal increments in potential can be checked by sketching in the perpendicular field lines. With the field lines forming curvilinear squares in the starting region, a correct distribution of the equipotentials is achieved when a grid of squares is maintained throughout the region. With some practice, it is possible to iterate between refinements of the equipotentials and the field lines until a satisfactory map of the solution is sketched.

Demonstration 7.6.2. Two-Dimensional Solution to Laplace's Equation by Means of Teledeltos Paper

For the mapping of *two-dimensional* fields, the conduction analog has the advantage that it is not necessary to make the electrodes and conductor "infinitely" long in the third dimension. Two-dimensional current distributions will result even in a thin-sheet conductor, provided that it has a conductivity that is large compared to its surroundings. Here again we exploit the boundary condition applying to the surfaces of the paper. As far as the fields inside the paper are concerned, a two-dimensional current distribution automatically meets the requirement that there be no current density normal to those parts of the paper bounded by air.

A typical field mapping apparatus is as simple as that shown in Fig. 7.6.3. The paper has the thickness Δ and a conductivity σ. The electrodes take the form of silver paint or copper tape put on the upper surface of the paper, with a shape simulating the electrodes of the actual system. Because the paper is so thin compared to dimensions of interest in the plane of the paper surface, the currents from the electrodes quickly assume an essentially uniform profile over the cross-section of the paper, much as suggested by the inset to Fig. 7.6.3.

In using the paper, it is usual to deal in terms of a surface resistance $1/\Delta\sigma$. The conductance of the plane parallel electrode system shown in Fig. 7.6.4 can be used to establish this parameter.

$$\frac{i}{v} = \frac{w\Delta\sigma}{S} \equiv G_p \Rightarrow \Delta\sigma = G_p\frac{S}{w} \tag{8}$$

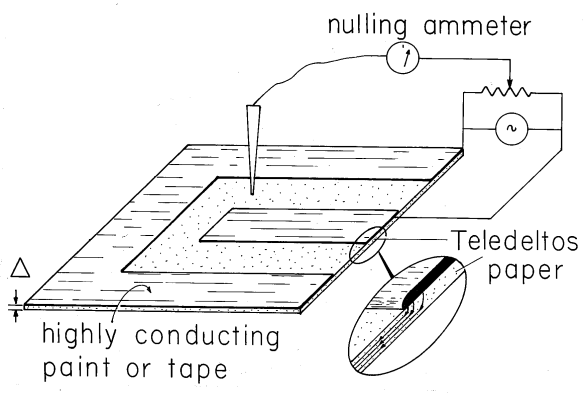

Fig. 7.6.3 Conducting paper with attached electrodes can be used to determine two-dimensional potential distributions.

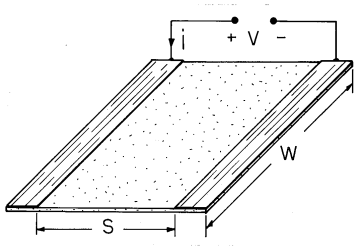

Fig. 7.6.4 Apparatus for determining surface conductivity $\Delta\sigma$ of paper used in experiment shown in Fig. 7.6.3.

The units are simply ohms, and $1/\Delta\sigma$ is the resistance of a square of the material having any sidelength. Thus, the units are commonly denoted as "ohms/square."

To associate a conductance as measured at the terminals of the experiment shown in Fig. 7.6.3 with the capacitance of a pair of electrodes having length l in the third dimension, note that the surface integrations used to define C and G reduce to

$$C = \frac{l}{v}\oint_C \epsilon\mathbf{E}\cdot d\mathbf{s}; \qquad G = \frac{\Delta}{v}\oint_C \sigma\mathbf{E}\cdot d\mathbf{s} \tag{9}$$

where the surface integrals have been reduced to line integrals by carrying out the integration in the third dimension. The ratio of these quantities follows in terms of the surface conductance $\Delta\sigma$ as

$$\frac{C}{G} = \frac{lk_1}{\Delta} = \frac{l\epsilon}{\Delta\sigma} \tag{10}$$

Here G is the conductance as actually measured using the conducting paper, and C is the capacitance of the two-dimensional capacitor it simulates.

In Chap. 9, we will find that magnetic field distributions as well can often be found by using the conduction analog.

TABLE 7.7.1
CHARGE RELAXATION TIMES OF TYPICAL MATERIALS

	$\sigma - \mathrm{S/m}$	ϵ/ϵ_o	$\tau_e - s$
Copper	5.8×10^{7}	1	1.5×10^{-19}
Water, distilled	2×10^{-4}	81	3.6×10^{-6}
Corn oil	5×10^{-11}	3.1	0.55
Mica	$10^{-11} - 10^{-15}$	5.8	$5.1 - 5.1 \times 10^{4}$

7.7 CHARGE RELAXATION IN UNIFORM CONDUCTORS

In a region that has uniform conductivity and permittivity, charge conservation and Gauss' law determine the unpaired charge density throughout the *volume* of the material, without regard for the boundary conditions. To see this, Ohm's law (7.1.7) is substituted for the current density in the charge conservation law, (7.0.3),

$$\nabla \cdot \sigma \mathbf{E} + \frac{\partial \rho_u}{\partial t} = 0 \tag{1}$$

and Gauss' law (6.2.15) is written using the linear polarization constitutive law, (6.4.3).

$$\nabla \cdot \epsilon \mathbf{E} = \rho_u \tag{2}$$

In a region where σ and ϵ are uniform, these parameters can be pulled outside the divergence operators in these equations. Substitution of $div\,\mathbf{E}$ found from (2) into (1) then gives the charge relaxation equation for ρ_u.

$$\boxed{\frac{\partial \rho_u}{\partial t} + \frac{\rho_u}{\tau_e} = 0; \qquad \tau_e \equiv \frac{\epsilon}{\sigma}} \tag{3}$$

Note that it has not been assumed that $\mathbf{E}$ is irrotational, so *the unpaired charge obeys this equation whether the fields are EQS or not.*

The solution to (3) takes on the same appearance as if it were an ordinary differential equation, say predicting the voltage of an RC circuit.

$$\rho_u = \rho_i(x, y, z)e^{-t/\tau_e} \tag{4}$$

However, (3) is a partial differential equation, and so the coefficient of the exponential in (4) is an arbitrary function of the spatial coordinates. The *relaxation time* τ_e has the typical values illustrated in Table 7.7.1.

The function $\rho_i(x, y, z)$ is the unpaired charge density when $t = 0$. Given any initial distribution, the subsequent distribution of ρ_u is given by (4). Once the

unpaired charge density has decayed to zero at a given point, it will remain zero. This is true regardless of the constraints on the surface bounding the region of uniform σ and ϵ. *Except for a transient that can only be initiated from very special initial conditions, the unpaired charge density in a material of uniform conductivity and permittivity is zero. This is true even if the system is not EQS.*

The following example is intended to help emphasize these implications of (3) and (4).

Example 7.7.1. Charge Relaxation in Region of Uniform σ and ϵ

In the region of uniform σ and ϵ shown in Fig. 7.7.1, the initial distribution of unpaired charge density is

$$\rho_i = \begin{cases} \rho_o; & r < a \\ 0; & a < r \end{cases} \tag{5}$$

where ρ_o is a constant.

It follows from (4) that the subsequent distribution is

$$\rho_u = \begin{cases} \rho_o e^{-t/\tau_e}; & r < a \\ 0; & a < r \end{cases}$$

As pictured in Fig. 7.7.1, the charge density in the spherical region $r < a$ remains uniform as it decays to zero with the time constant τ_e. The charge density in the surrounding region is initially zero and remains so throughout the transient.

Charge conservation implies that there must be a current density in the material surrounding the initially charged spherical region. Yet, according to the laws used here, there is never a net unpaired charge density in that region. This is possible because in Ohmic conduction, there are at least two types of charges involved. In the uniformly conducting material, one or both of these migrate in the electric field caused by the net charge [in accordance with (7.1.5)] while exactly neutralizing each other so that $\rho_u = 0$ (7.1.6).

Net Charge on Bodies Immersed in Uniform Materials[2]. The integral charge relaxation law, (1.5.2), applies to the net charge within any volume containing a medium of constant ϵ and σ. If an initially charged particle finds itself suspended in a fluid having uniform σ and ϵ, this charge must decay with the charge relaxation time constant τ_e.

Demonstration 7.7.1. Relaxation of Charge on Particle in Ohmic Conductor

The pair of plane parallel electrodes shown in Fig. 7.7.2 is immersed in a semi-insulating liquid, such as corn oil, having a relaxation time on the order of a second. Initially, a metal particle rests on the lower electrode. Because this particle makes electrical contact with the lower electrode, application of a potential difference results in charge being induced not only on the surfaces of the electrodes but on the surface of the particle as well. At the outset, the particle is an extension of the lower

[2] This subsection is not essential to the material that follows.

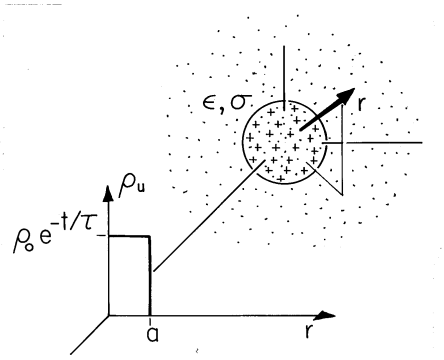

Fig. 7.7.1 Within a material having uniform conductivity and permittivity, initially there is a uniform charge density ρ_u in a spherical region, having radius a. In the surrounding region the charge density is given to be initially zero and found to be always zero. Within the spherical region, the charge density is found to decay exponentially while retaining its uniform distribution.

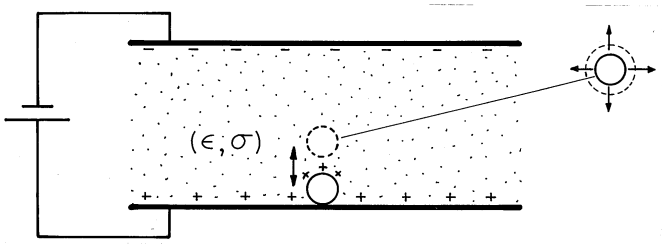

Fig. 7.7.2 The region between plane parallel electrodes is filled by a semi-insulating liquid. With the application of a constant potential difference, a metal particle resting on the lower plate makes upward excursions into the fluid. [See footnote 1.]

electrode. Thus, there is an electrical force on the particle that is upward. Note that changing the polarity of the voltage changes the sign of both the particle charge and the field, so the force is always upward.

As the voltage is raised, the electrical force outweighs the net gravitational force on the particle and it lifts off. As it separates from the lower electrode, it does so with a net charge sufficient to cause the electrical force to start it on its way toward charges of the opposite sign on the upper electrode. However, if the liquid is an Ohmic conductor with a relaxation time shorter than that required for the particle to reach the upper electrode, the net charge on the particle decays, and the upward electrical force falls below that of the downward gravitational force. In this case, the particle falls back to the lower electrode without reaching the upper one. Upon contacting the lower electrode, its charge is renewed and so it again lifts off. Thus, the particle appears to bounce on the lower electrode.

By contrast, if the oil has a relaxation time long enough so that the particle can reach the upper electrode before a significant fraction of its charge is lost, then the particle makes rapid excursions between the electrodes. Contact with the upper electrode results in a charge reversal and hence a reversal in the electrical force as well.

The experiment demonstrates that as long as a particle is electrically isolated

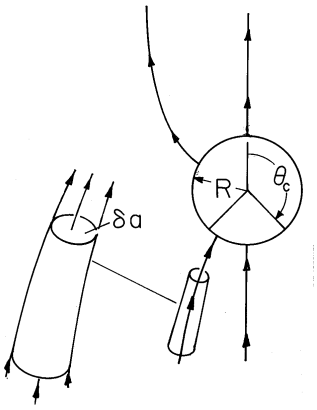

Fig. 7.7.3 Particle immersed in an initially uniform electric field is charged by unipolar current of positive ions following field lines to its surface. As the particle charges, the "window" over which it can collect ions becomes closed.

in an Ohmic conductor, its charge will decay to zero and will do so with a time constant that is the relaxation time ϵ/σ. According to the Ohmic model, once the particle is surrounded by a uniformly conducting material, it cannot be given a net charge by any manipulation of the potentials on electrodes bounding the Ohmic conductor. The charge can only change upon contact with one of the electrodes.

We have found that a particle immersed in an *Ohmic* conductor can only discharge. This is true even if it finds itself in a region where there is an externally imposed conduction current. By contrast, the next example illustrates how a *unipolar* conduction process can be used to charge a particle. The ion-impact charging (or field charging) process is put to work in electrophotography and air pollution control.

Example 7.7.2. Ion-Impact Charging of Macroscopic Particles

The particle shown in Fig. 7.7.3 is itself perfectly conducting. In its absence, the surrounding region is filled by an un-ionized gas such as air permeated by a uniform z-directed electric field. Positive ions introduced at $z \to -\infty$ then give rise to a unipolar current having a density given by the unipolar conduction law, (7.1.8). With the introduction of the particle, some of the lines of electric field intensity can terminate on the particle. These carry ions to the particle. Other lines originate on the particle and it is assumed that there is no mechanism for the particle surface to initiate ions that would then carry charge away from the particle along these lines. Thus, as the particle intercepts some of the ion current, it charges up.

Here the particle-charging process is described as a sequence of steady states. The charge conservation equation (7.0.3) obtained by using the unipolar conduction law (7.1.8) then requires that

$$\nabla \cdot (\mu\rho\mathbf{E}) = 0 \tag{6}$$

Thus, the "field" $\rho\mathbf{E}$ (consisting of the product of the charge density and the electric field intensity) forms flux tubes. These have walls tangential to $\mathbf{E}$ and incremental

cross-sectional areas $\delta\mathbf{a}$, as illustrated in Figs.7.7.3 and 2.7.5, such that $\rho\mathbf{E}\cdot\delta\mathbf{a}$ remains constant.

As a second approximation, it is assumed that the dominant sources for the electric field are on the boundaries, either on the surface of the particle or at infinity. Thus, the ions in the volume of the gas are low enough in concentration so that their volume charge density makes a negligible contribution to the electric field intensity. At each point in the volume of the gas,

$$\nabla\cdot\epsilon_o\mathbf{E}\approx 0 \tag{7}$$

From this statement of Gauss' law, it follows that the $\mathbf{E}$ lines also form flux tubes along which $\mathbf{E}\cdot\delta\mathbf{a}$ is conserved. Because both $\mathbf{E}\cdot\delta\mathbf{a}$ and $\rho\mathbf{E}\cdot\delta\mathbf{a}$ are constant along a given $\mathbf{E}$ line, it is necessary that the charge density ρ be constant along these lines. This fact will now be used to calculate the current of ions to the particle.

At a given instant in the charging process, the particle has a net charge q. Its surface is an equipotential and it finds itself in an electric field that is uniform at infinity. The distribution of electric field for this situation was found in Example 5.9.2. Lines of electric field intensity terminate on the southern end of the sphere over the range $\pi\geq\theta\geq\theta_c$, where θ_c is shown in Figs. 7.7.3 and 5.9.2. In view of the unipolar conduction law, these lines carry with them a current density. Thus, there is a net current into the particle given by

$$i=\int_{\theta_c}^{\pi}-\mu\rho E_r(r=R,\theta)(2\pi R\sin\theta R d\theta) \tag{8}$$

Because ρ is constant along an electric field line and ρ is uniform far from the charge-collecting particles, it is a constant over the surface of integration.

It follows from (5.9.13) that the normal electric field needed to evaluate (8) is

$$E_r=-\frac{\partial\Phi}{\partial r}\Big|_{r=R}=3E_a\cos\theta+\frac{q}{4\pi\epsilon_o R^2} \tag{9}$$

Substitution of (9) into (8) gives

$$i=-\mu\rho 6\pi R^2E_a\int_{\theta_c}^{\pi}\Big(\cos\theta+\frac{q}{q_c}\Big)\sin\theta d\theta \tag{10}$$

where, as in Example 5.9.2, $q_c=12\pi\epsilon_o R^2E_a$ and

$$-\cos\theta_c=\frac{q}{q_c} \tag{11}$$

Remember, θ_c is the angle at which the radial electric field switches from being outward to inward. Thus, it is a function of the amount of charge on the particle. Substitution of (11) into (10) and some manipulation gives the net current to the particle as

$$i=\frac{q_c}{\tau_i}\Big(1-\frac{q}{q_c}\Big)^2 \tag{12}$$

where $\tau_i=4\epsilon_o/\mu\rho$.

From (10) it is clear that the current depends on the particle charge. As charge accumulates on the particle, the angle θ_c increases and so the southern surface over

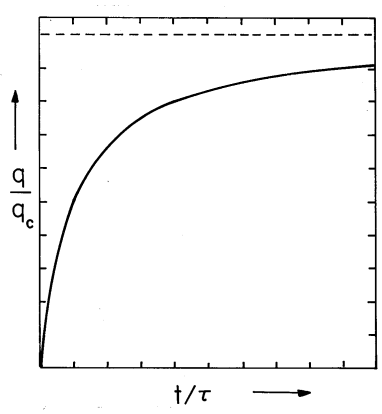

Fig. 7.7.4 Normalized particle charge as a function of normalized time. The saturation charge q_c and charging time τ are given after (10) and (12), respectively.

which electric field lines terminate decreases. By the time $q = q_c$, the collection surface is zero and, as implied by (12), the current goes to zero.

If the charging process is slow enough to be viewed as a sequence of stationary states, the current given by (12) is equal to the rate of increase of the particle charge.

$$\frac{dq}{dt} = i \Rightarrow \frac{d(q/q_c)}{d(t/\tau_i)} = \left(1 - \frac{q}{q_c}\right)^2 \tag{13}$$

Divided by what is on the right and multiplied by the denominator on the left, this expression can be integrated.

$$\int_0^{q/q_c} \frac{d\left(\frac{q'}{q_c}\right)}{\left(1 - \frac{q'}{q_c}\right)^2} = \int_0^{t/\tau_i} d\left(\frac{t}{\tau_i}\right) \tag{14}$$

The result is a charging law that is not exponential but rather

$$\frac{q}{q_c} = \frac{t/\tau_i}{1 + t/\tau_i} \tag{15}$$

This charging transient is shown in Fig. 7.7.4. By contrast with a particle placed in a conduction current that is Ohmic, a particle subjected to a unipolar current will charge up to the saturation charge q_c. Note that the charging time, $\tau_i = 4\epsilon_o/\mu\rho$, again takes the form of ϵ divided by a "conductivity."

Demonstration 7.7.2. Electrostatic Precipitation

Once dust, smoke, or fume particles are charged, they can be subjected to an electric field and pulled out of the gas in which they are interspersed. In large precipitators used to filter combustion gases before they are released from a stack, the charging and precipitation processes are carried out in one region. The apparatus of Fig. 7.7.5 illustrates this process.

A fine wire is stretched along the axis of a grounded conducting cylinder having a radius of 5–10 cm. With the wire at a voltage of 10–30 kv, a hissing sound gives

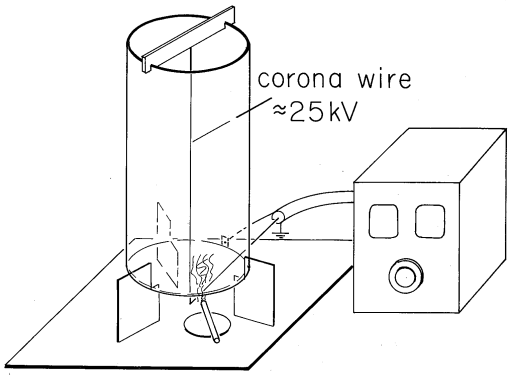

Fig. 7.7.5 Electrostatic precipitator consisting of fine wire at high voltage relative to surrounding conducting transparent coaxial cylinder. Ions created in corona discharge in the immediate vicinity of the wire follow field lines toward outer wall, some terminating on smoke particles. Once charged by the mechanism described in Example 7.7.2, the smoke particles are precipitated on the outer wall.

evidence of ionization of the air in the immediate vicinity of the wire. This corona discharge provides positive and negative ion pairs adjacent to the wire. If the wire is positive, some of the positive ions are drawn out of this region and migrate to the cylindrical outer wall. Thus, outside the corona discharge region there is a unipolar conduction current of the type postulated in Example 7.7.2. The ion mobility is typically $(1 \rightarrow 2) \times 10^{-4}$ (m/s)/(v/m), while the field is on the order of 5×10^5 v/m, so the ion velocity (7.1.3) is in the range of $50 - 100$ m/s.

Smoke particles, mixed with air rising through the cylinder, can be seen to be removed from the gas within a second or so. Large polyethylene particles dropped in from the top can be more readily seen to collect on the walls. In a practical precipitator, the collection electrodes are periodically rapped so that chunks of the collected material drop into a hopper below.

Most of the time required to clear the air of smoke is spent by the particle in migrating to the wall after it has been charged. The charging time constant τ_i is typically only a few milliseconds.

This demonstration further emphasizes the contrast between the behavior of a macroscopic particle when immersed in an Ohmic conductor, as in the previous demonstration, and when subjected to unipolar conduction. A particle immersed in a unipolar "conductor" becomes charged. In a uniform Ohmic conductor, it can only discharge.

7.8 ELECTROQUASISTATIC CONDUCTION LAWS FOR INHOMOGENEOUS MATERIALS

In this section, we extend the discussion of transients to situations in which the electrical permittivity and Ohmic conductivity are arbitrary functions of space.

$$\epsilon = \epsilon(\mathbf{r}), \qquad \sigma = \sigma(\mathbf{r}) \tag{1}$$

Distributions of these parameters, as exemplified in Figs. 6.5.1 and 7.2.3, might be uniform, piece-wise uniform, or smoothly nonuniform. The specific examples falling into these categories answer three questions.

(a) Where does the unpaired charge density, found in Sec. 7.7, tend to accumulate when it disappears from a region having uniform properties.
(b) With the unpaired charge density determined by the self-consistent EQS laws, what is the equation governing the potential distribution throughout the volume of interest?
(c) What boundary and initial conditions make the solutions to this equation unique?

The laws studied in this section and exemplified in the next describe both the perfectly insulating limit of Chap. 6 and the conduction dominated limit of Secs. 7.1–7.6. More important, as suggested in Sec. 7.0, they describe how these limiting situations are related in EQS systems.

Evolution of Unpaired Charge Density. With a nonuniform conductivity distribution, the statement of charge conservation and Ohm's law expressed by (7.7.1) becomes

$$\sigma\nabla\cdot\mathbf{E}+\mathbf{E}\cdot\nabla\sigma+\frac{\partial\rho_u}{\partial t}=0 \tag{2}$$

Similarly, with a nonuniform permittivity, Gauss' law as given by (7.7.2) becomes

$$\epsilon\nabla\cdot\mathbf{E}+\mathbf{E}\cdot\nabla\epsilon=\rho_u \tag{3}$$

Elimination of $\nabla\cdot\mathbf{E}$ between these equations gives an expression that is the generalization of the charge relaxation equation, (7.7.3).

$$\frac{\partial\rho_u}{\partial t}+\frac{\rho_u}{(\epsilon/\sigma)}=-\mathbf{E}\cdot\nabla\sigma+\frac{\sigma}{\epsilon}\mathbf{E}\cdot\nabla\epsilon \tag{4}$$

Wherever the electric field has a component in the direction of a gradient of σ or ϵ, the unpaired charge density can be present and can be temporally increasing or decreasing. If a steady state has been established, in the sense that time rates of change are negligible, the charge distribution is given by (4), because then, $\partial\rho_u/\partial t=0$. Note that this is the distribution of (7.2.8) that prevails for steady conduction. We can therefore expect that the charge density found to disappear from a region of uniform properties in Sec. 7.7 will reappear at surfaces of discontinuity of σ and ϵ or in regions where ϵ and σ vary smoothly.

Electroquasistatic Potential Distribution. To evaluate (4), the self-consistent electric field intensity is required. With the objective of determining that field, Gauss' law, (7.7.2), is used to eliminate ρ_u from the charge conservation statement, (7.7.1).

$$\nabla\cdot\sigma\mathbf{E}+\frac{\partial}{\partial t}(\nabla\cdot\epsilon\mathbf{E})=0 \tag{5}$$

For the first time in the analysis of charge relaxation, we now introduce the electroquasistatic approximation

$$\nabla \times \mathbf{E} \simeq 0 \Rightarrow \mathbf{E} = -\nabla\Phi \tag{6}$$

and (5) becomes the desired expression governing the evolution of the electric potential.

$$\boxed{\nabla \cdot \left(\sigma\nabla\Phi + \frac{\partial}{\partial t}\epsilon\nabla\Phi\right) = 0} \tag{7}$$

Uniqueness. Consider now the initial and boundary conditions that make solutions to (7) unique. Suppose that throughout the volume V, the initial charge distribution is given as

$$\rho_u(\mathbf{r}, t = 0) = \rho_i(\mathbf{r}) \tag{8}$$

and that on the surface S enclosing this volume, the potential is a given function of time

$$\Phi = \Phi_i(\mathbf{r}, t) \text{ on } S \text{ for } t \geq 0. \tag{9}$$

Thus, when $t = 0$, the initial distribution of electric field intensity satisfies Gauss' law. The initial potential distribution satisfies the same law as for regions occupied by perfect dielectrics.

$$\nabla \cdot \epsilon\nabla\Phi_i = -\rho_i \tag{10}$$

Given the boundary condition of (9) when $t = 0$, it follows from Sec. 5.2 that the initial distribution of potential is uniquely determined.

Is the subsequent evolution of the field uniquely determined by (7) and the initial and boundary conditions? To answer this question, we will take a somewhat more formal approach than used in Sec. 5.2 but nevertheless use the same reasoning. Supose that there are two solutions, $\Phi = \Phi_a$ and $\Phi = \Phi_b$, that satisfy (7) and the same initial and boundary conditions.

Equation (7) is written first with $\Phi = \Phi_a$ and then with $\Phi = \Phi_b$. With $\Phi_d \equiv \Phi_a - \Phi_b$, the difference between these two equations becomes

$$\nabla \cdot \left[\sigma\nabla\Phi_d + \frac{\partial}{\partial t}(\epsilon\nabla\Phi_d)\right] = 0 \tag{11}$$

Multiplication of (11) by Φ_d and integration over the volume V gives

$$\int_V \Phi_d \nabla \cdot \left[\sigma\nabla\Phi_d + \frac{\partial}{\partial t}(\epsilon\nabla\Phi_d)\right] dv = 0 \tag{12}$$

The objective in the following manipulation is to turn this integration either into one over positive definite quantities or into an integration over the surface S, where the boundary conditions determine the potential. The latter is achieved if the integrand can be expressed as a divergence. Thus, the vector identity

$$\nabla \cdot \psi\mathbf{A} = \psi\nabla \cdot \mathbf{A} + \mathbf{A} \cdot \nabla\psi \tag{13}$$

is used to write (12) as

$$\int_V \nabla \cdot \left[\Phi_d\left(\sigma\nabla\Phi_d + \frac{\partial}{\partial t}\epsilon\nabla\Phi_d\right)\right]dv - \int_V \left(\sigma\nabla\Phi_d + \frac{\partial}{\partial t}\epsilon\nabla\Phi_d\right)\cdot\nabla\Phi_d dv = 0 \tag{14}$$

and then Gauss' theorem converts the first integral to one over the surface S enclosing V.

$$\oint_S \Phi_d\left(\sigma\nabla\Phi_d + \frac{\partial}{\partial t}\epsilon\nabla\Phi_d\right)\cdot d\mathbf{a} - \int_V \left[\sigma|\nabla\Phi_d|^2 + \frac{\partial}{\partial t}\left(\frac{1}{2}\epsilon|\nabla\Phi_d|^2\right)\right]dv = 0 \tag{15}$$

The conversion of (12) to (15) is an example of a three-dimensional integration by parts. The surface integral is analogous to an evaluation at the endpoints of a one-dimensional integral.

If both Φ_a and Φ_b satisfy the same condition on S, namely (9), then the difference potential is zero on S for all $0 \leq t$. Thus, the surface integral in (15) vanishes. We are left with the requirement that for $0 \leq t$,

$$\frac{d}{dt}\int_V \frac{1}{2}\epsilon|\nabla\Phi_d|^2 dv = -\int_V \sigma|\nabla\Phi_d|^2 dv \tag{16}$$

Because both Φ_a and Φ_b satisfy the same initial conditions, Φ_d must initially be zero. Thus, for $\nabla\Phi_d$ to change to a nonzero value from zero, the derivative on the left must be positive. However, the integral on the right can only be zero or negative. Thus, Φ_d must stay zero for all time. We conclude that the fields found using (7), the initial condition of (8), and boundary conditions of (9) are unique.

7.9 CHARGE RELAXATION IN UNIFORM AND PIECE-WISE UNIFORM SYSTEMS

Configurations composed of subregions where the material has uniform properties are already familiar from Secs. 6.6 and 7.5. The conductivity and permittivity are then step functions of position, and the terms on the right in (7.8.4) are spatial impulses. Thus, the charge density tends to accumulate at interfaces between regions and is represented by a surface charge density.

We consider first the evolution of the potential distribution in a region having uniform properties. With the inhomogeneities represented by the continuity conditions, the discussion is then extended to piece-wise uniform configurations.

Fields in Regions Having Uniform Properties. Where ϵ and σ are uniform, (7.8.7) becomes

$$\nabla^2\left[\frac{\partial\Phi}{\partial t} + \frac{\Phi}{(\epsilon/\sigma)}\right] = 0 \tag{1}$$

This expression is satisfied either if the potential obeys the relaxation equation

$$\frac{\partial \Phi_p}{\partial t} + \frac{\Phi_p}{(\epsilon/\sigma)} = 0 \tag{2}$$

or if it satisfies Laplace's equation

$$\nabla^2 \Phi_h = 0 \tag{3}$$

In general, the potential is a linear combination of these solutions.

$$\Phi = \Phi_p + \Phi_h \tag{4}$$

The potential satisfying (2) is that associated with the relaxation of the charge density initially distributed in the volume of the material. We can think of this as being a particular solution, because the divergence of the associated electric displacement $\mathbf{D} = \epsilon \mathbf{E} = -\epsilon \nabla \Phi_p$ gives the unpaired charge density, (7.7.4), at each point in the volume V for $t > 0$. The solutions Φ_h to Laplace's equation can then be used to make the sum of the two solutions satisfy the boundary conditions.

Given that the initial charge density throughout the volume is $\rho_i(\mathbf{r})$, the subsequent distribution is given by (7.7.4). One particular solution for the potential that then satisfies Poisson's equation throughout the volume follows from evaluating the superposition integral [(4.5.3) with $\epsilon_o \to \epsilon$] over that volume.

$$\Phi_p = \int_{V'} \frac{\rho_i(\mathbf{r}')}{4\pi\epsilon|\mathbf{r} - \mathbf{r}'|} dv' e^{-t/(\epsilon/\sigma)} \tag{5}$$

Note that this potential indeed satisfies (2) and the initial conditions on the charge density in the volume. Of course, the integral could be extended to charges outside the volume V, and the particular solution would be equally valid.

The solutions to Laplace's equation make it possible to make the total potential satisfy boundary conditions. Because an initial distribution of volume charge density cannot be initiated by means of boundary electrodes, the decay of an initial charge density is not usually of interest. The volume potential is most often simply a solution to Laplace's equation. Before delving into these more common examples, consider one that illustrates the more general situation.

Example 7.9.1. Potential Associated with Relaxation of Volume Charge

In Example 7.7.1, the decay of charge having a spherical distribution in space was described. This could be done without regard for boundary constraints. To determine the associated potential, we stipulate the nature of the boundary surrounding the uniform material in which the charge is initially embedded.

The uniform material fills the upper half-space and is bounded in the plane $z = 0$ by a perfect conductor constrained to zero potential. As shown in Fig. 7.9.1, when $t = 0$, there is an initial distribution of charge density that is uniform and of

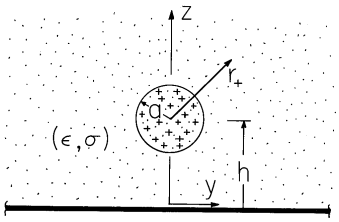

Fig. 7.9.1 Infinite half-space of material having uniform conductivity and permittivity is bounded from below by a perfectly conducting plate. When $t = 0$, there is a uniform charge density in a spherical region.

density ρ_o throughout a spherical region of radius a centered at $z = h$ on the z axis, where $h > a$.

In terms of a spherical coordinate system centered on the z axis at $z = h$, a particular solution for the potential follows from the integral form of Gauss' law, much as in Example 1.3.1. With r_+ denoting the radial distance from the center of the spherical region,

$$\Phi_p = \begin{cases} \frac{3a^2 - r_+^2}{6\epsilon}\rho_o e^{-t/\tau}; & r_+ < a \\ \frac{a^3\rho_o}{3\epsilon r_+}e^{-t/\tau}; & a < r_+ \end{cases} \tag{6}$$

where $r_+ = [x^2 + y^2 + (z-h)^2]^{1/2}$ and $\tau \equiv \epsilon/\sigma$.

Note that this potential satisfies (2) and the initial condition but does not satisfy the zero potential condition at $z = 0$. To satisfy the latter, we add a potential that is a solution to Laplace's equation, (3), everywhere in the upper half-space. This is the potential associated with an image charge density $-\rho_o exp(-t/\tau)$ distributed uniformly over a spherical region of radius a centered at $z = -h$.

$$\Phi_h = \frac{-a^3\rho_o}{3\epsilon r_-}e^{-t/\tau} \tag{7}$$

where $r_- = [x^2 + y^2 + (z+h)^2]^{1/2}, \quad z > 0$.

Thus, the total potential $\Phi = \Phi_p + \Phi_h$ that satisfies both the initial conditions and boundary conditions for $0 < t$ is

$$\Phi = \begin{cases} \frac{3a^2 - r_+^2}{6\epsilon}\rho_o e^{-t/\tau} - \frac{a^3\rho_o}{3\epsilon r_-}e^{-t/\tau}; & r_+ < a \\ \frac{a^3\rho_o}{3\epsilon}\left(\frac{1}{r_+} - \frac{1}{r_-}\right)e^{-t/\tau}; & a < r_+ \end{cases} \tag{8}$$

At each instant in time, the potential distribution is the same as if the charge and its image were static. As the charge relaxes, so does its image. Note that the charge relaxes to the boundary without producing a net charge density anywhere outside the spherical region where the charge was initiated.

Continuity Conditions in Piece-Wise Uniform Systems. Where the material properties undergo step discontinuities, the differential equations are represented by continuity conditions. The one representing the condition that the field be irrotational, (7.8.6), is the same as that in Sec. 5.3.

$$\mathbf{n} \times (\mathbf{E}^a - \mathbf{E}^b) = 0 \Leftrightarrow \Phi^a - \Phi^b = 0 \tag{9}$$

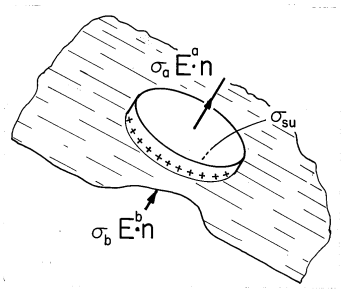

Fig. 7.9.2 Incremental volume for writing charge conservation boundary condition.

The continuity condition representing Gauss' law, (7.7.2), is also familiar (6.2.16).

$$\boxed{\sigma_{su} = \mathbf{n} \cdot (\epsilon_a \mathbf{E}^a - \epsilon_b \mathbf{E}^b)} \tag{10}$$

The continuity condition representing charge conservation, (7.7.1), is (1.5.12). With the current density expressed in terms of Ohm's law, this continuity condition becomes

$$\boxed{\mathbf{n} \cdot (\sigma_a \mathbf{E}^a - \sigma_b \mathbf{E}^b) + \frac{\partial}{\partial t}\sigma_{su} = 0} \tag{11}$$

For the incremental volume of Fig. 7.9.2, this continuity condition requires that if the conduction current entering the volume from region (b) exceeds that leaving to region (a), there must be an increasing surface charge density within the volume.

The fact that we are solving a second-order differential equation, (7.8.7), suggests that there are really only two continuity conditions. Thus, Gauss' continuity condition only serves to relate the field to the unknown surface charge density, and the combination of (10) and (11) comprise one continuity condition.

$$\mathbf{n} \cdot (\sigma_a \mathbf{E}^a - \sigma_b \mathbf{E}^b) + \frac{\partial}{\partial t}\mathbf{n} \cdot (\epsilon_a \mathbf{E}^a - \epsilon_b \mathbf{E}^b) = 0 \tag{12}$$

This continuity condition and the one on the tangential field or potential, (9), are needed to splice together solutions representing fields in piece-wise uniform configurations.

The following example illustrates how the time dependence of the continuity condition allows the fields and charge distribution to evolve from the distributions for perfect dielectrics described in the latter part of Chap. 6 to the steady conduction distributions discussed in the first part of this chapter.

Example 7.9.2. Maxwell's Capacitor

A configuration that brings out the roles of polarization and conduction in the field evolution while avoiding geometric complications is shown in Fig. 7.9.3. The space

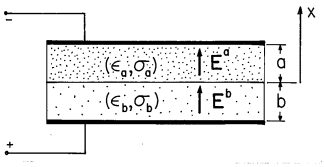

Fig. 7.9.3 Maxwell's capacitor.

between perfectly conducting parallel plates is filled by layers of material. The one above has thickness a, permittivity ϵ_a, and conductivity σ_a, while for the one below, these parameters are b, ϵ_b, and σ_b, respectively. When $t = 0$, a switch is closed and the potential V of a battery is applied across the two electrodes. Initially, there is no unpaired charge between the electrodes either in the volume or on the interface.

The electrodes are assumed long enough so that the fringing can be neglected and the fields in each of the materials taken as uniform.

$$\mathbf{E} = \mathbf{i_x} \begin{cases} E_a(t); & 0 < x < a \\ E_b(t); & -b < x < 0 \end{cases} \tag{13}$$

The linear potential associated with this distribution satisfies Laplace's equation, (3). Because there is no initial charge density in the volumes of the layers, the particular part of the potential, the solution to (2), is zero.

The voltage source imposes the condition that the line integral of the electric field between the plates must be equal to $v(t)$.

$$\int_{-b}^{a} E_x dx = v(t) = aE_a + bE_b \tag{14}$$

Because the layers are conducting, they respond to the application of the voltage with conduction currents. Since the currents differ, they cause a time rate of change of unpaired surface charge density at the interface between the layers, as expressed by (12).

$$(\sigma_a E_a - \sigma_b E_b) + \frac{d}{dt}(\epsilon_a E_a - \epsilon_b E_b) = 0 \tag{15}$$

Note that the boundary conditions on tangential $\mathbf{E}$ at the electrode surfaces and at the interface are automatically satisfied.

Given the driving voltage, these last two expressions comprise two equations in the two unknowns E_a and E_b. Thus, the solution to (14) for E_b and substitution into (15) gives a first-order differential equation for the field response in the upper layer.

$$(b\epsilon_a + a\epsilon_b)\frac{dE_a}{dt} + (b\sigma_a + a\sigma_b)E_a = \sigma_b v + \epsilon_b \frac{dv}{dt} \tag{16}$$

In particular, consider the response to a step in voltage, $v = Vu_{-1}(t)$. The drive on the right in (16) then consists of a step and an impulse. The impulse must be matched by an impulse on the left. That is, the field E_a also undergoes a step change when $t = 0$. To identify the magnitude of this step, integrate (16) from 0^- to 0^+.

$$\begin{aligned}(b\epsilon_a + a\epsilon_b)\int_{0^-}^{0^+} \frac{dE_a}{dt}dt + (b\sigma_a + a\sigma_b)\int_{0^-}^{0^+} E_a dt \\ = \sigma_b \int_{0^-}^{0^+} v dt + \epsilon_b \int_{0^-}^{0^+} \frac{dv}{dt}dt\end{aligned} \tag{17}$$

The result is a relationship between the jumps in voltage and in field.

$$\left(\epsilon_a + \frac{a}{b}\epsilon_b\right)[E_a(0^+) - E_a(0^-)] = \frac{\epsilon_b}{b}[v(0^+) - v(0^-)] \tag{18}$$

Because $v(0^-) = 0$ and $E_a(0^-) = 0$, it follows that

$$E_a(0^+) = \epsilon_b \frac{V}{b\epsilon_a + a\epsilon_b} \tag{19}$$

For $t > 0$, the particular plus homogeneous solution to (16) is

$$E_a = \sigma_b \frac{V}{b\sigma_a + a\sigma_b} + Ae^{-t/\tau} \tag{20}$$

where

$$\tau \equiv \frac{b\epsilon_a + a\epsilon_b}{b\sigma_a + a\sigma_b}.$$

The coefficient A is adjusted to make E_a meet the initial condition given by (19). Thus, the field transient in the upper layer is found to be

$$E_a = \frac{\sigma_b V}{(b\sigma_a + a\sigma_b)}(1 - e^{-t/\tau}) + \frac{\epsilon_b V}{(b\epsilon_a + a\epsilon_b)}e^{-t/\tau} \tag{21}$$

It follows from (14) that the field in the lower layer is then

$$E_b = \frac{V}{b} - \frac{a}{b}E_a \tag{22}$$

The unpaired surface charge density, (10), follows from these fields.

$$\sigma_{su} = \frac{V(\sigma_b\epsilon_a - \sigma_a\epsilon_b)}{(b\sigma_a + a\sigma_b)}(1 - e^{-t/\tau}) \tag{23}$$

The field and unpaired surface charge density transients are shown in Fig. 7.9.4. The curves are drawn to depict a lower layer that has a somewhat greater permittivity and a much greater conductivity than the upper layer. Just after the step in voltage, when $t = 0^+$, the surface charge density remains zero. Thus, the electric fields are at first what they would be if the layers were regarded as perfectly insulating dielectrics. As the surface charge accumulates, these fields approach values consistent with steady conduction. The limiting surface charge density approaches a saturation value that could be found by first evaluating the steady conduction fields and then finding σ_{su}. Note that this surface charge can be positive or negative. With the lower region much more conducting than the upper one ($\sigma_b\epsilon_a \gg \sigma_a\epsilon_b$) the surface charge is positive. In this case, the field ends up tending to be shielded out of the lower layer.

Piece-wise continuous configurations can often be represented by capacitor-resistor networks. An exact circuit representation of Maxwell's capacitor is shown in Fig. 7.9.5. The voltages across the capacitors are simply $v_a = E_a a$ and $v_b = E_b b$. In the circuit, the surface charge density given by (23) is the sum of the net charge per unit area on the lower plate of the top capacitor and that on the upper plate of the lower capacitor.

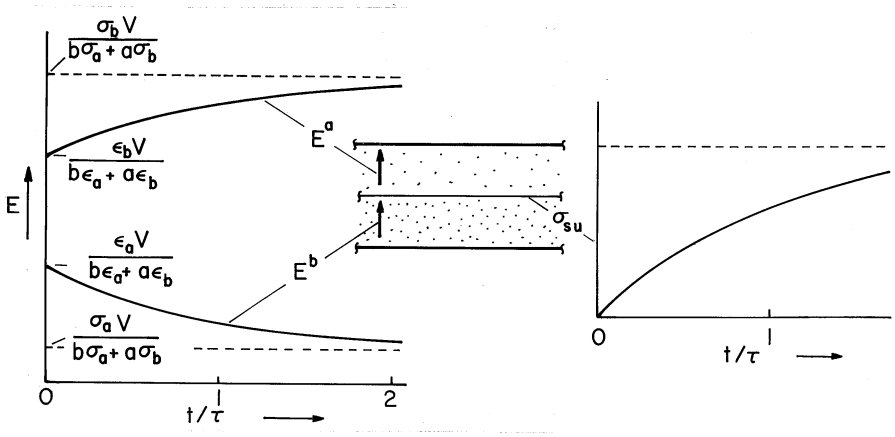

Fig. 7.9.4 With a step in voltage applied to the plane parallel configuration of Fig. 7.9.3, the electric field intensity above and below the interface responds as shown on the left, while the unpaired surface charge density has the time dependence shown on the right.

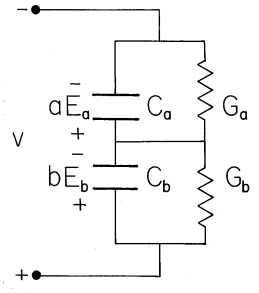

Fig. 7.9.5 Maxwell's capacitor, Fig. 7.9.3, is exactly equivalent to the circuit shown.

Nonuniform Fields in Piece-Wise Uniform Systems. We continue now to consider examples with no initial charge density in the regions having uniform conductivity and dielectric constant. Since it is not possible to establish a charge density in these regions by means of boundary constraints, this is almost always the situation in practice. The field distributions in the uniform subregions have potentials that satisfy Laplace's equation, (3). These are "spliced" together at the interfaces between regions and constrained at boundaries by conditions that vary with time. The continuity conditions vary with time to account for the accumulation of unpaired charge at the interfaces between regions.

Maxwell's capacitor, Example 7.9.2, illustrates most features of the surface charge relaxation process. The response to a step function of voltage across an electrode pair is at first the field distribution of a system of perfect dielectrics, as developed in Chap. 6. After many charge relaxation times, steady conduction prevails, and the fields are as described in Sec. 7.5. In the remainder of this section, configurations will be considered that, by contrast to Maxwell's capacitor, have fields that change their shape as the relaxation process evolves.

The interplay of polarization and conduction processes is also evident in the

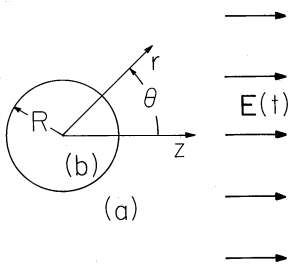

Fig. 7.9.6 A spherical material with conductivity σ_b and permittivity ϵ_b is surrounded by a material with conductivity and permittivity (σ_a, ϵ_a). An electric field $E(t)$ that is uniform far from the sphere is applied.

sinusoidal steady state response of a system. Just as the Maxwell capacitor has short-time and long-time responses dominated by the "capacitors" and "resistors," respectively, the high-frequency and low-frequency responses are dominated by polarization and conduction, respectively. This too will now be illustrated.

Example 7.9.3. Spherical Semi-insulating Material Embedded in a Second Material Stressed by Uniform Electric Field

An electric field intensity $E(t)$ is imposed on a material having permittivity and conductivity (ϵ_a, σ_a), perhaps by means of plane parallel electrodes. At the origin of a spherical coordinate system embedded in this material is a spherical region having permittivity and conductivity (ϵ_b, σ_b) and radius R, as shown in Fig. 7.9.6. Limiting cases include a conducting sphere surrounded by free space ($\epsilon_a = \epsilon_o$, $\sigma_a = 0$) or an insulating spherical cavity surrounded by a conducting material ($\sigma_b = 0$).

In each of the regions, the potential must satisfy Laplace's equation. From our experience with the potentials for perfect dielectric and for steady conduction configurations, we can expect that the boundary conditions can be satisfied using combinations of uniform and dipole fields. With the understanding that the coefficients $A(t)$ and $B(t)$ are functions of time, the solutions to Laplace's equation are therefore postulated to take the form

$$\Phi = \begin{cases} -E(t)r\cos\theta + A(t)\frac{\cos\theta}{r^2}; & r > R \\ B(t)r\cos\theta; & r < R \end{cases} \tag{24}$$

Note that the uniform part of the exterior field has been matched at $r \to \infty$ to the given driving field.

Continuity of the tangential electric field at $r = R$, (9), requires that these potential functions match at $r = R$.

$$\Phi^a(r = R) = \Phi^b(r = R) \tag{25}$$

Conservation of charge, with the surface charge density represented using Gauss' law, (12), makes the further requirement that

$$(\sigma_a E_r^a - \sigma_b E_r^b) + \frac{\partial}{\partial t}(\epsilon_a E_r^a - \epsilon_b E_r^b) = 0 \tag{26}$$

In substituting the potentials of (24) into these two conditions, no derivatives with respect to θ are taken, so each term has the θ dependence $\cos(\theta)$. It is for this

reason that such a simple solution can be used to satisfy the continuity conditions. Substitution into (25) relates the coefficients

$$-ER + \frac{A}{R^2} = BR \Rightarrow B = -E + \frac{A}{R^3} \tag{27}$$

and with this relation used to eliminate B, substitution into (26) results in a differential equation for $A(t)$, with $E(t)$ as a driving function.

$$(2\epsilon_a + \epsilon_b)\frac{dA}{dt} + (2\sigma_a + \sigma_b)A = (\sigma_b - \sigma_a)R^3E(t) + (\epsilon_b - \epsilon_a)R^3\frac{dE}{dt} \tag{28}$$

Step Response. Note that expression (28) has the same form as that for Maxwell's capacitor, (16). The procedure leading to the field response to a step function of applied field, $E = E_o u_{-1}(t)$, is therefore identical to that illustrated in Example 7.9.2. In fact, comparison of these equations makes it clear that the required solution, given that there were no initial fields (when $t = 0^-$), is

$$A = E_o R^3 \left[\frac{\sigma_b - \sigma_a}{2\sigma_a + \sigma_b}(1 - e^{-t/\tau}) + \frac{\epsilon_b - \epsilon_a}{2\epsilon_a + \epsilon_b}e^{-t/\tau} \right] \tag{29}$$

where the relaxation time $\tau = (2\epsilon_a + \epsilon_b)/(2\sigma_a + \sigma_b)$. The coefficient B follows from (27). Thus, the potential of (24) is determined for $t \geq 0$.

$$\Phi = -E_o R\cos\theta \begin{cases} \frac{r}{R} + \left[\frac{\sigma_a - \sigma_b}{2\sigma_a + \sigma_b}(1 - e^{-t/\tau}) + \frac{\epsilon_a - \epsilon_b}{2\epsilon_a + \epsilon_b}e^{-t/\tau} \right](\frac{R}{r})^2; & R < r \\ \frac{r}{R}\left[1 + \frac{\sigma_a - \sigma_b}{2\sigma_a + \sigma_b}(1 - e^{-t/\tau}) + \frac{\epsilon_a - \epsilon_b}{2\epsilon_a + \epsilon_b}e^{-t/\tau} \right]; & r < R \end{cases} \tag{30}$$

The accumulation of unpaired surface charge at $r = R$ accounts for the redistribution of potential with time. It follows from (10) that

$$\sigma_{su} = \epsilon_a E_r^a - \epsilon_b E_r^b = 3E_o \frac{(\epsilon_a\sigma_b - \epsilon_b\sigma_a)}{(2\sigma_a + \sigma_b)}(1 - e^{-t/\tau})\cos\theta \tag{31}$$

Thus, the unpaired surface charge density accumulates at the poles of the sphere, exponentially approaching a saturation value at a rate determined by the relaxation time τ. *Just after the field is turned on, this surface charge density is zero and the field distribution should be that for a uniform field applied to perfect dielectrics.* Indeed, evaluated when $t = 0$, (30) gives the potential for perfect dielectrics. In the opposite extreme, *where many relaxation times have passed so that the exponentials in (30) are negligible, the potential assumes the distribution for steady conduction.*

A graphical portrayal of this field transient is given in Fig. 7.9.7. The case shown was chosen because it involves a drastic redistribution of the field as time progresses. The spherical region is highly conducting compared to its surroundings, but the exterior material is highly polarizable compared to the spherical region. Thus, just after the switch is closed, the field lines tend to be trapped in the outer region. As time progresses and conduction rules, these lines tend to pass through

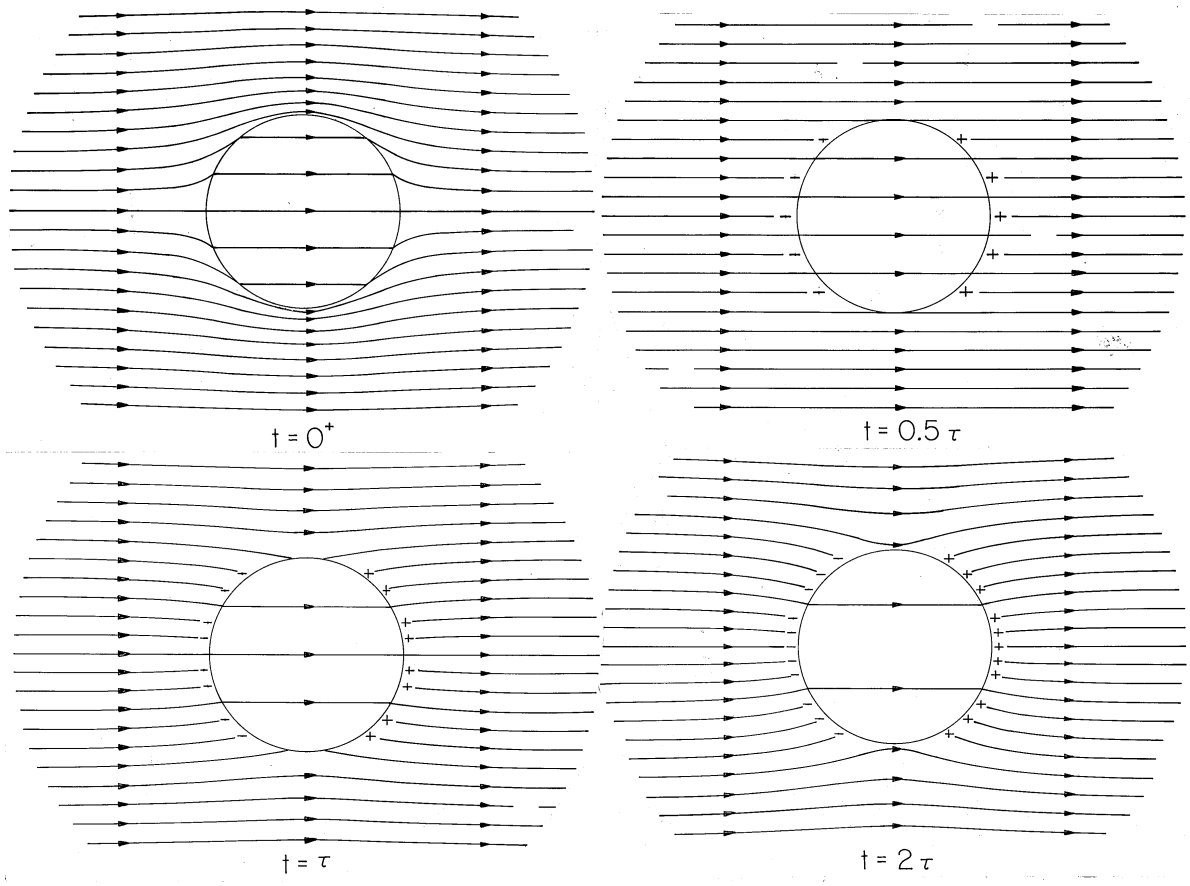

Fig. 7.9.7 Evolution of the *displacement flux density* **D** in and around the sphere of Fig. 7.9.6 and of σ_{su} in response to the application of a step in applied field. The sphere is more conducting than its surroundings ($\sigma_a/\sigma_b = 0.2$), while the outer region has a greater permittivity than the inner one, $\epsilon_a/\epsilon_b = 5$. Thus, when the distribution of **D** is determined by the polarization just after the field is applied, the field lines tend to be trapped in the outer region. By the time $t = 0.5\,\tau$, enough σ_{su} has been induced to cancel the field associated with σ_{sp}, and the *electric field intensity* is essentially uniform. In the final state, conduction alone determines the distribution of **E**. However, it is **D** that is shown in the figure, so, in fact, the permittivities do contribute to the final relative intensities.

the highly conducting sphere. The temporal scale of the transient is determined by the relaxation time τ.

Sinusoidal Steady State Response. Consider now the sinusoidal steady state that results from applying the uniform field

$$E(t) = E_p \cos \omega t = Re E_p e^{j\omega t} \tag{32}$$

As in dealing with ac circuits, where the currents and voltages are also solutions to constant coefficient ordinary differential equations, the response is now assumed to have the same frequency ω as the drive but to have a yet to be determined amplitude and phase represented by the complex coefficients A and B.

$$A(t) = Re\hat{A}e^{j\omega t}; \qquad B(t) = Re\hat{B}e^{j\omega t} \tag{33}$$

Substitution of (32) and (33a) into (28) gives an expression that can be solved for $\hat{A}$ in terms of the drive, E_p.

$$\hat{A} = \frac{[(\sigma_b - \sigma_a) + j\omega(\epsilon_b - \epsilon_a)]}{(2\sigma_a + \sigma_b) + j\omega(2\epsilon_a + \epsilon_b)} R^3 E_p \tag{34}$$

In turn, the complex amplitude B follows from this result and (27).

$$\hat{B} = -E_p + \frac{\hat{A}}{R^3} = -3E_p \frac{(\sigma_a + j\omega\epsilon_a)}{(2\sigma_a + \sigma_b) + j\omega(2\epsilon_a + \epsilon_b)} \tag{35}$$

Now, with the amplitudes in (31) and (32) given by these expressions, the sinusoidal steady state fields postulated with (24) are determined.

$$\Phi = -Re\, E_p R \cos\theta e^{j\omega t} \begin{cases} \frac{r}{R} + \left[\frac{(\sigma_a - \sigma_b) + j\omega(\epsilon_a - \epsilon_b)}{(2\sigma_a + \sigma_b) + j\omega(2\epsilon_a + \epsilon_b)}\right](\frac{R}{r})^2; & r > R \\ 3\frac{r}{R}\frac{(\sigma_a + j\omega\epsilon_a)}{(2\sigma_a + \sigma_b) + j\omega(2\epsilon_a + \epsilon_b)}; & R > r \end{cases} \tag{36}$$

The surface charge density associated with these fields is then

$$\sigma_{su} = Re \frac{3E_p(\sigma_b\epsilon_a - \sigma_a\epsilon_b)}{(2\sigma_a + \sigma_b) + j\omega(2\epsilon_a + \epsilon_b)} \cos\theta e^{j\omega t} \tag{37}$$

With the frequency rather than the time as the parameter, these expressions can be interpreted analogously to the step function response, (30) and (31). In the high-frequency limit, where

$$\frac{\omega(2\epsilon_a + \epsilon_b)}{2\sigma_a + \sigma_b} \equiv \omega\tau \gg 1; \qquad \omega\left[\frac{(\epsilon_a - \epsilon_b)}{(\sigma_a - \sigma_b)}\right] \gg 1 \tag{38}$$

the conductivity terms become negligible in (36), the coefficients $\hat{A}$ and $\hat{B}$ become independent of frequency and real. Thus, the fields are in temporal phase with the applied field and sinusoidally varying versions of what would be found if the materials were assumed to be perfect dielectrics. *If the frequency is high compared to the reciprocal charge relaxation times, the field distributions are the same as they would be just after a step in applied field* [when $t = 0^+$ in (30)].

With the inequalities of (38) reversed, the terms involving the permittivity in (36) are negligible, the coefficients $\hat{A}$ and $\hat{B}$ are again real and hence the fields are just as they would be for stationary conduction except that they vary sinusoidally with time. Thus, *in the low frequency limit, the fields are sinusoidally varying versions of the steady conduction fields* that prevail long after a step in applied field [(30) in the limit $t \to \infty$].

These high- and low-frequency limits are consistent with the frequency dependence of the unpaired surface charge density, given by (37). At low frequencies, this surface charge density varies sinusoidally in or out of phase with the applied field and with an amplitude consistent with steady conduction. As the frequency is made to greatly exceed the reciprocal relaxation time, the magnitude of this charge falls to zero. In this high-frequency limit, there is insufficient time during one cycle for significant charge to relax to the spherical interface. Thus, at high frequencies the fields become the same as if the unpaired charge density were ignored and the dielectrics assumed to be perfectly insulating.

In the two demonstrations that close this section, an obvious objective is the association of the previous example with practical situations. The approximations used to rederive the relevant fields cast further light on the physical processes at work.

Demonstration 7.9.1. Capacitively Induced Fields in a Person in the Vicinity of a High-Voltage Power Line

A person standing under a conventional power line, as in Fig. 7.9.8a, is subject to a 60 Hz alternating electric field intensity that is typically 5×10^4 v/m. In response to this field, body currents are induced. Common experience suggests that these are not large enough to create discomfort, but are the currents appreciable enough to be of long-term medical concern?

In the bare-handed maintenance of power lines, a person is brought to within arms length of the line by an insulated hoist, as shown in Fig. 7.9.8b. Without shielding, the body is in this case subjected to much more intense fields, perhaps 5×10^5 v/m. For the first person proving out this technique, the estimation of fields and currents within the body was of considerable interest.

To the layman, these imposed fields seem to imply that a body one meter in length would be subject to a voltage difference of 50 kV at the ground and 500 kV near the line. However, as we will now illustrate, surrounded by air, the body does an excellent job of shielding out the electric field.

The hemispherical conductor resting on a ground plane, shown in Fig. 7.9.9, is a model for an individual on (and in electrical contact with) the ground. In the experiment, the hemisphere is jello, molded to have the radius R and having a conductivity essentially that of the salt water used in its making. (To obtain the physiological conductivity of 0.2 S/m, unflavored gelatine is made using 0.02 M NaCl, a solution of 1.12 grams/liter.)

Presumably, the potential in and around the hemisphere is given by (30). The $z = 0$ plane is at zero potential for the spherical region described, and so the potential applies equally well to the hemisphere on the ground plane. Parameters are $(\epsilon_a, \sigma_a) = (\epsilon_o, 0)$ in the air and $(\epsilon_b, \sigma_b) = (\epsilon, \sigma)$ in the hemisphere. A conductivity typical of physiological tissue is $\sigma = .2$ S/m. As a result, the charge relaxation time based on the permittivity of the body ($\epsilon_b = 81\epsilon_o$) and the conductivity of the body is extremely short, $\tau = 4 \times 10^{-9}$ s. This makes it possible to approximate the potential distribution using the two simple steps that follow.

First, because the charge can relax to the surface in a time that is far shorter than $1/\omega$, and because the hemisphere is surrounded by material that has far less conductivity, as far as the field in the air is concerned, its surface is an equipotential.

$$\Phi_a(r = R) \simeq 0 \tag{39}$$

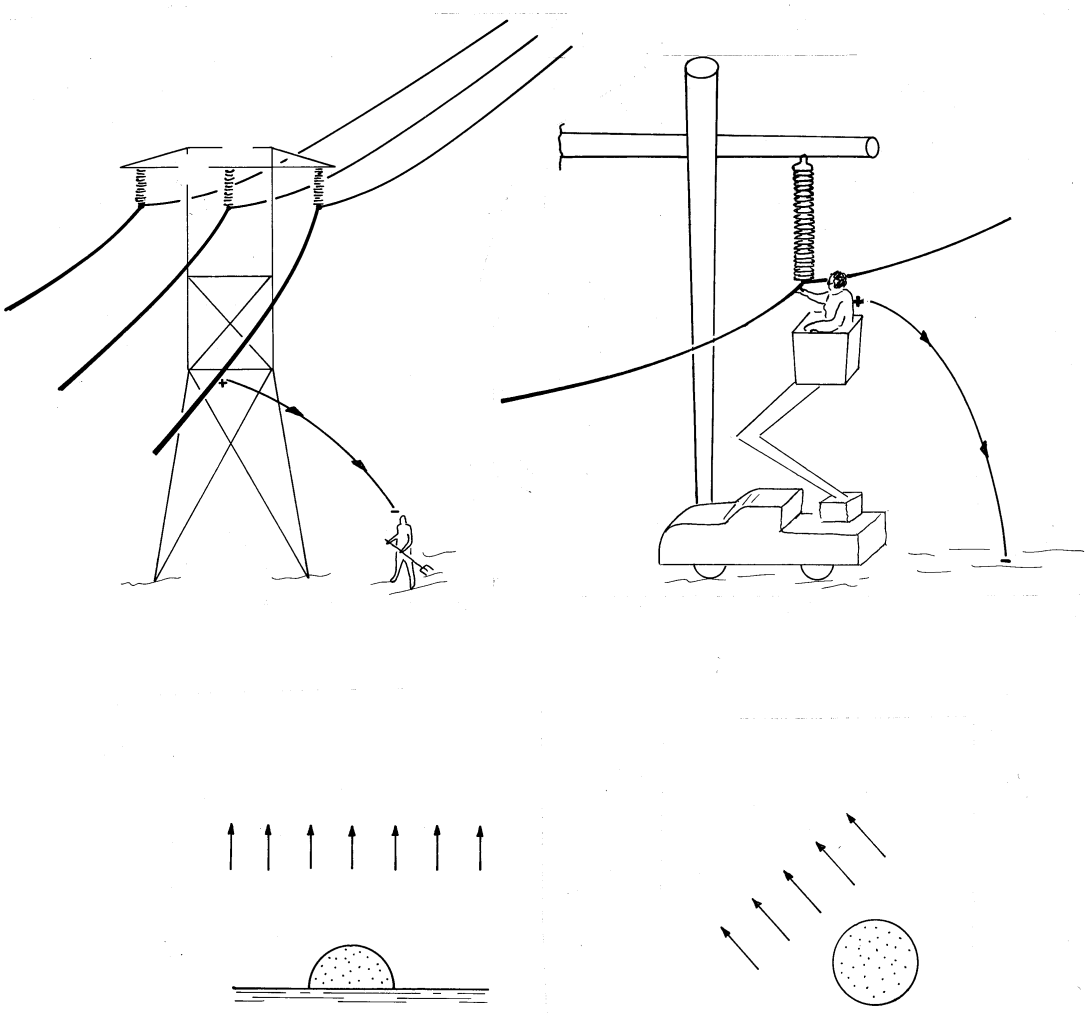

Fig. 7.9.8 (a) Person in vicinity of power line terminates lines of electric field intensity and hence is subject to currents associated with induced charge. The electric field intensity at the ground is as much as 5×10^4 V/m. (b) Worker carrying out "bare-handed maintenance" is subject to field that depends greatly on shielding provided, but can be 5×10^5 V/m or more. (c) Hemispherical model for person on ground in (a). (d) Spherical model for person near line without shielding, (b).

Thus, the potential distribution can be written by inspection [or by recourse to (5.9.7)] as

$$\Phi_a \simeq -E_p R \cos \omega t \left[\left(\frac{r}{R} \right) - \left(\frac{R}{r} \right)^2 \right] \cos \theta \tag{40}$$

Because of the short relaxation time and high conductivity for the sphere relative to the air, the surface charge density is essentially determined by the exterior field.

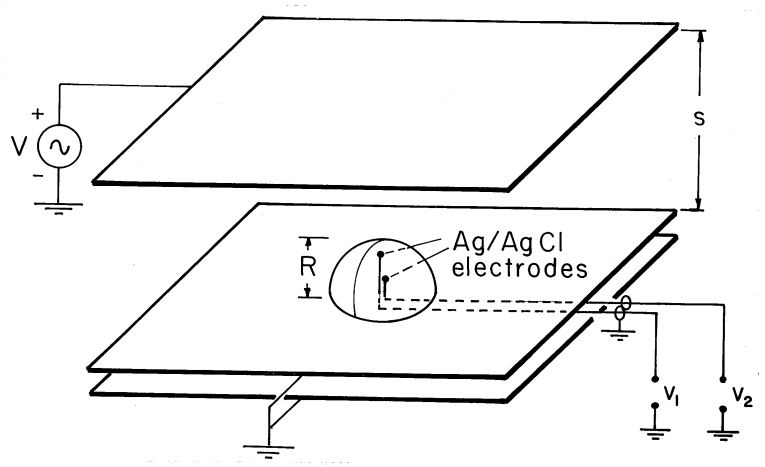

Fig. 7.9.9 Demonstration of currents induced in flesh-simulating hemisphere by field applied in surrounding air.

Thus, the conservation of charge continuity condition, (12), is approximately

$$\sigma E_r^b(r=R) \simeq \frac{\partial}{\partial t}[\epsilon_o E_r^a(r=R)] \tag{41}$$

The rate of change of the surface charge density on the right in this expression has already been determined, so the expression serves to evaluate the normal conduction current density just inside the hemispherical surface.

$$E_r^b(r=R) = -\frac{3\omega\epsilon_o E_p}{\sigma}\sin\omega t\cos\theta \tag{42}$$

In the interior region, the potential is uniform and thus takes the form $Br\cos(\theta)$. Evaluation of the coefficient B by using (42) then gives the approximate potential distribution within the hemisphere.

$$\Phi^b \simeq \frac{3\omega\epsilon_o}{\sigma}E_p r\ \cos\theta\sin\omega t = \frac{3\omega\epsilon_o}{\sigma}E_p z\sin\omega t \tag{43}$$

In retrospect, note that the potentials given by (40) and (43) are obtained by taking the appropriate limit of the potential obtained without making approximations, (36).

Inside the hemisphere, the conditions for essentially steady conduction prevail. Thus, the potential predicted by (43) is probed by means of metal spheres (Ag/AgCl electrodes) embedded in the jello and connected to an oscilloscope through insulated wires. Inside the hemisphere, surface charge stored on the surfaces of the insulated wires has a minor effect on the current distribution.

Typical experimental values for a 250 Hz excitation are $R = 3.8$ cm, $s = 12.7$ cm, $v = 565$ V peak, and $\sigma = 0.2$ S/m. With the probes located at $z = 2.86$ cm and $z = 0.95$ cm, the measured potentials are 25 μV peak and 10 μV peak, respectively. With the given parameters, (43) gives 26.5 μV peak and 8.8 μV peak, respectively.

What are the typical current densities that would be induced in a person in the vicinity of a power line? According to (41), for the person on the ground in a

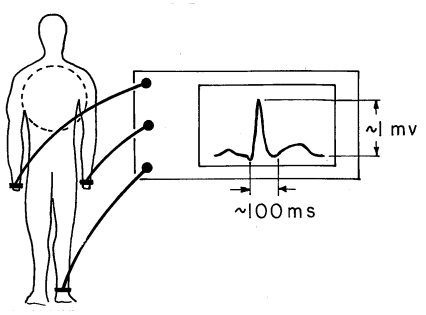

Fig. 7.9.10 Configuration for an electrocardiogram, including voltages typically generated at body periphery by the heart.

field of 5×10^4 V/m (Fig. 7.9.8a), the current density is $J_z = \sigma E_z = 0.05\mu\text{A/cm}^2$. For the person doing bare-handed maintenance where the field is perhaps 5×10^5 V/m (Fig. 7.9.8b), the model is a sphere in a uniform field (Fig. 7.9.8d). The current density is again given by (43), $J_z = \sigma E_z = 0.5\mu\text{A/cm}^2$.

Of course, the geometry of a person is not spherical. Thus, it can be expected that the field will concentrate more in the actual situation than for the hemispherical or spherical models. The approximations introduced in this demonstration would greatly simplify the development of a numerical model.

Have we found estimates of current densities suggesting danger, especially for the maintenance worker? Physiological systems are far too complex for there to be a simple answer to this question. However, matters are placed in some perspective by recognizing that currents of diverse origins exist in the body so long as it lives. In the next demonstration, electrocardiogram potentials are used to estimate current densities that result from the muscular contractions of the heart. The magnitude of the current density found there will lend some perspective to that determined here.

The approximate analysis introduced in support of the previous demonstration is an example of the "inside-outside" viewpoint introduced in Sec. 7.5. The exterior insulating region, where the field was applied, was "inside," while the interior conducting region was "outside." The following demonstration continues this theme with a contrasting example, where the excitation is in the conducting region.

Demonstration 7.9.2. Currents Induced by the Heart

The configuration for taking an electrocardiogram is typically as shown in Fig. 7.9.10. With care taken to balance out 60 Hz signals induced in each of the electrodes by external fields, the electrical signals induced by the muscle contractions in the heart are easily measured using a conventional oscilloscope. In practice, many electrodes are used so that detailed information on the distribution of the muscle contractions can be discerned.

Here we simply represent the heart by a dipole source of current at the center of a conducting sphere, somewhat as depicted in Figs. 7.9.10 and 7.9.11. Relatively little current is induced in the limbs, so that potentials measured at the extremities roughly reflect the potentials on the surface of the equivalent sphere. Given that typical potential differences are on the order of millivolts, what current dipole moment can we attribute to the heart, and what are the typical current densities in its neighborhood?

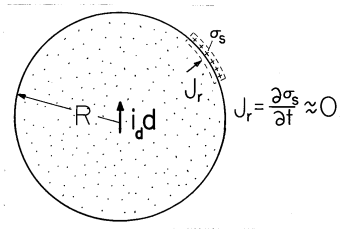

Fig. 7.9.11 Body and heart modeled by spherical conductor and dipole current.

With the heart represented by a current source of dipole moment $i_p d$ at the center of the spherical "torso," the electric potential at the origin approaches that for the dipole current source, (7.3.9).

$$\Phi_b(r \to 0) \to \frac{i_p d}{4\pi\sigma}\frac{\cos\theta}{r^2} \tag{44}$$

At the surface $r = R$, the spherical body is being surrounded by an insulator. Thus, again using Fig. 7.9.11, any normal conduction current must be accounted for by the accumulation of surface charge. Because the relaxation time is so short compared to the $1s$ period typical of the heart, the current density associated with the buildup of surface charge is extremely small. As a result, the current distribution inside the sphere is as though the normal current density at $r = R$ were zero.

$$\frac{\partial\Phi_b}{\partial r}(r = R) \simeq 0 \tag{45}$$

Thus, the potential within the body is fully determined without regard for constraints from the surrounding region. The solution to Laplace's equation that satisfies these last two conditions is

$$\Phi_b \simeq \frac{i_p d}{4\pi\sigma R^2}\left[\left(\frac{R}{r}\right)^2 + 2\left(\frac{r}{R}\right)\right]\cos\theta \tag{46}$$

Because the potential is continuous at $r = R$, the potential on the surface of the "torso" follows from evaluation of this expression at $r = R$.

$$\Phi_a(r = R) = \Phi_b(r = R) = \frac{3(i_p d)}{4\pi\sigma R^2}\cos\theta \tag{47}$$

Thus, given that the potential difference between $\theta = 45$ degrees and $\theta = 135$ degrees is 1 mV, that $R = 25$ cm, and that $\sigma = 0.2$ S/m, it follows from (47) that the peak current dipole moment of the heart is 3.7×10^{-5} A - m.

Typical current densities can now be found using (46) to evaluate the electric field intensity. For example, the current density at the radius $R/2$ just above the dipole source is

$$\begin{aligned} J_z &= \sigma E_z\left(r = \frac{R}{2},\ \theta = 0\right) = \frac{7(i_p d)}{2\pi R^3} \\ &= 2.6 \times 10^{-3}\mathrm{A/m^2} = 0.26\,\mu\mathrm{A/cm^2} \end{aligned} \tag{48}$$

Note that at the particular position selected the current density exceeds with some margin that to which the maintenance worker is subjected in the previous demonstration.

To begin to correlate the state and function of the heart with electrocardiograms, it is necessary to represent the heart by a current dipole that not only has a special temporal signature but rotates with time as well[1,2]. Unfortunately, much of the medical literature on the subject takes the analogy between electric dipoles (Sec.4.4) and current dipoles (Sec. 7.3) literally. The heart is described as an electric dipole[2], which it certainly is not. If it were, its fields would be shielded out by the surrounding conducting flesh.

REFERENCES

[1] R. Plonsey, **Bioelectric Phenomena**, McGraw-Hill Book Co., N.Y. (1969), p. 205.

[2] A. C. Burton, **Physiology and Biophysics of the Circulation**, Year Book Medical Pub., Inc., Chicago, Ill. 2nd ed., pp. 125-138.

7.10 SUMMARY

This chapter can be divided into three parts. In the first, Sec. 7.1, conduction constitutive laws are related to the average motions of microscopic charge carriers. Ohm's law, as it relates the current density $\mathbf{J}_u$ to the electric field intensity $\mathbf{E}$

$$\mathbf{J}_u = \sigma\mathbf{E} \tag{1}$$

is found to describe conduction in certain materials which are constituted of at least one positive and one negative species of charge carrier. As a reminder that the current density can be related to field variables in many ways other than Ohm's law, the unipolar conduction law is also derived in Sec. 7.1, (7.1.8). But in this chapter and those to follow, the conduction law (1) is used almost exclusively.

The second part of this chapter, Secs. 7.2–7.6, is concerned with "steady" conduction. A summary of the differential laws and corresponding continuity conditions is given in Table 7.10.1. Under steady conditions, the unpaired charge density is determined from the last expressions in the table after the first two have been used to determine the electric potential and field intensity.

In the third part of this chapter, Secs. 7.7–7.9, the dynamics of EQS systems is developed and exemplified. The laws used to determine the electric potential and field intensity, given by the first two lines in Table 7.10.2, are valid for frequencies and characteristic times that are arbitrary relative to electrical relaxation times, provided those times are themselves long compared to times required for an electromagnetic wave to propagate through the system. The last expressions identify how the unpaired charge density is relaxing under dynamic conditions.

In EQS systems, the magnetic induction makes a negligible contribution and the electric field intensity is essentially irrotational. Thus, $\mathbf{E}$ is represented by

TABLE 7.10.1
SUMMARY OF LAWS FOR STEADY STATE OHMIC CONDUCTION

	Differential Law	Eq. No.	Continuity Condition	Eq. No.
Faraday's Law	$\nabla \times \mathbf{E} \simeq 0 \Leftrightarrow \mathbf{E} = -\nabla\Phi$	(7.0.1)	$\Phi^a - \Phi^b = 0$	(7.2.10)
Charge conservation	$\nabla \cdot \sigma\mathbf{E} = s$	(7.2.2) (7.3.1)	$\mathbf{n} \cdot (\sigma_a\mathbf{E}^a - \sigma_b\mathbf{E}^b) = J_s$	(7.2.9) (7.3.4)
Unpaired charge distribution	$\rho_u = -\frac{\epsilon}{\sigma}\mathbf{E} \cdot \nabla\sigma + \mathbf{E} \cdot \nabla\epsilon$	(7.2.8)	$\sigma_{su} = \mathbf{n} \cdot \epsilon_a\mathbf{E}^a\left(1 - \frac{\epsilon_b\sigma_a}{\epsilon_a\sigma_b}\right)$	(7.2.12)

TABLE 7.10.2
SUMMARY OF EQS LAWS FOR INHOMOGENEOUS OHMIC MEDIA

	Differential Law	Eq. No.	Continuity Condition	Eq. No.
Faraday's law	$\mathbf{E} = -\nabla\Phi$	(7.0.1)	$\Phi^a - \Phi^b = 0$	(7.2.10)
Charge conservation, Ohm's law, and Gauss' law	$\nabla \cdot \left[\sigma\mathbf{E} + \frac{\partial}{\partial t}(\epsilon\mathbf{E})\right] = s$	(7.8.5) (7.3.2)	$\mathbf{n} \cdot (\sigma_a\mathbf{E}^a - \sigma_b\mathbf{E}^b) + \frac{\partial}{\partial t}\mathbf{n} \cdot (\epsilon_a\mathbf{E}^a - \epsilon_b\mathbf{E}^b) = J_s$	(7.9.12) (7.3.4)
Relaxation of unpaired charge density	$\frac{\partial\rho_u}{\partial t} + \frac{\rho_u}{\epsilon/\sigma} = -\mathbf{E} \cdot \nabla\sigma + \frac{\sigma}{\epsilon}\mathbf{E} \cdot \nabla\epsilon$	(7.8.4)	$\frac{\partial\sigma_{su}}{\partial t} + \mathbf{n} \cdot (\sigma_a\mathbf{E}^a - \sigma_b\mathbf{E}^b) = 0$	(7.9.11)

$-grad\,(\Phi)$ in both Table 7.10.1 and Table 7.10.2. In the EQS approximation, neglecting the magnetic induction is tantamount to ignoring the finite transit time effects of electromagnetic waves. This we saw in Chap. 3 and will see again in Chaps. 14 and 15.

In MQS systems, fields may be varying so slowly that the effect of magnetic induction on the current flow is again ignorable. In that case, the laws of Table 7.10.1 are once again applicable. So it is that the second part of this chapter is a logical base from which to begin the next chapter. At least under steady conditions we already know how to predict the distribution of the current density, the source of the magnetic field intensity.

How rapidly can MQS fields vary without having the magnetic induction come into play? We will answer this question in Chap. 10.

PROBLEMS

7.1 Conduction Constitutive Laws

7.1.1 In a metal such as copper, where each atom contributes approximately one conduction electron, typical current densities are the result of electrons moving at a surprisingly low velocity. To estimate this velocity, assume that each atom contributes one conduction electron and that the material is copper, where the molecular weight $M_o = 63.5$ and the mass density is $\rho = 8.9 \times 10^3 kg/m^3$. Thus, the density of electrons is approximately $(A_o/M_o)\rho$, where $A_o = 6.023 \times 10^{26}$ molecules/kg-mole is Avogadro's number. Given σ from Table 7.1.1, what is the mobility of the electrons in copper? What electric field intensity is required to drive a current density of 1 amp/cm^2? What is the electron velocity?

7.2 Steady Ohmic Conduction

7.2.1* The circular disk of uniformly conducting material shown in Fig. P7.2.1 has a dc voltage v applied to its surfaces at $r = a$ and $r = b$ by means of perfectly conducting electrodes. The other boundaries are interfaces with free space. Show that the resistance $R = ln(a/b)/2\pi\sigma d$.

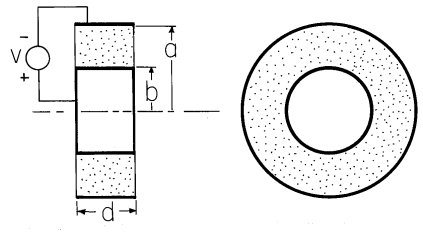

Fig. P7.2.1

7.2.2 In a spherical version of the resistor shown in Fig. P7.2.1, a uniformly conducting material is connected to a voltage source v through spherical perfectly conducting electrodes at $r = a$ and $r = b$. What is the resistance?

7.2.3* By replacing $\epsilon \rightarrow \sigma$, resistors are made to have the same geometry as shown in Fig. P6.5.1. In general, the region between the plane parallel perfectly conducting electrodes is filled by a material of conductivity $\sigma = \sigma(x)$. The boundaries of the conductor that interface with the surrounding free space have normals that are either in the x or the z direction.

(a) Show that even if d is large compared to l and c, $\mathbf{E}$ between the plates is $(v/d)\mathbf{i_y}$.

(b) If the conductor is piece-wise uniform, with sections having conductivities σ_a and σ_b of width a and b, respectively, as shown in Fig. P6.5.1a, show that the conductance $G = c(\sigma_b b + \sigma_a a)/d$.

(c) If $\sigma = \sigma_a(1 + x/l)$, show that $G = 3\sigma_a cl/2d$.

7.2.4 A pair of uniform conductors form a resistor having the shape of a circular cylindrical half-shell, as shown in Fig. P7.2.4. The boundaries at $r = a$ and $r = b$, and in planes parallel to the paper, interface with free space. Show that for steady conduction, all boundary conditions are satisfied by a simple piece-wise continuous potential that is an exact solution to Laplace's equation. Determine the resistance.

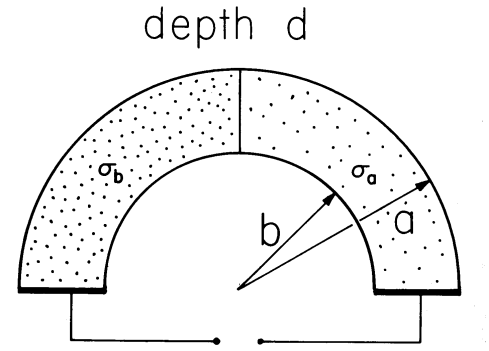

Fig. P7.2.4

7.2.5* The region between the planar electrodes of Fig. 7.2.4 is filled with a material having conductivity $\sigma = \sigma_o/(1 + y/a)$, where σ_o and a are constants. The permittivity ϵ is uniform.

(a) Show that $G = A\sigma_o/d(1 + d/2a)$.

(b) Show that $\rho_u = \epsilon Gv/A\sigma_o a$.

7.2.6 The region between the planar electrodes of Fig. 7.2.4 is filled with a uniformly conducting material having permittivity $\epsilon = \epsilon_a/(1 + y/a)$.

(a) What is G?

(b) What is ρ_u in the conductor?

7.2.7* A section of a spherical shell of conducting material with inner radius b and outer radius a is shown in Fig. P7.2.7. Show that if $\sigma = \sigma_o(r/a)^2$, the conductance $G = 6\pi(1 - \cos\alpha/2)ab^3\sigma_o/(a^3 - b^3)$.

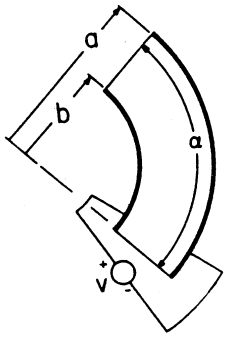

Fig. P7.2.7

7.2.8 In a cylindrical version of the geometry shown in Fig. P7.2.7, the material between circular cylindrical outer and inner electrodes of radii a and b, respectively, has conductivity $\sigma = \sigma_o(a/r)$. The boundaries parallel to the page interface free space and are a distance d apart. Determine the conductance G.

7.3 Distributed Current Sources and Associated Fields

7.3.1* An infinite half-space of uniformly conducting material in the region $y > 0$ has an interface with free space in the plane $y = 0$. There is a point current source of I amps located at $(x, y, z) = (0, h, 0)$ on the y axis. Using an approach analogous to that used in Prob. 6.6.5, show that the potential inside the conductor is

$$\Phi_a = \frac{I}{4\pi\sigma\sqrt{x^2 + (y-h)^2 + z^2}} + \frac{I}{4\pi\sigma\sqrt{x^2 + (y+h)^2 + z^2}}. \qquad (a)$$

Now that the potential of the interface is known, show that the potential in the free space region outside the conductor, where $y < 0$, is

$$\Phi_b = \frac{2I}{4\pi\sigma\sqrt{x^2 + (y-h)^2 + z^2}} \qquad (b)$$

7.3.2 The half-space $y > 0$ is of uniform conductivity while the remaining space is insulating. A uniform line current source of density K_l (A/m) runs parallel to the plane $y = 0$ along the line $x = 0,\ y = h$.

(a) Determine Φ in the conductor.
(b) In turn, what is Φ in the insulating half-space?

7.3.3* A two-dimensional dipole current source consists of uniform line current sources $\pm K_l$ have the spacing d. The cross-sectional view is as shown in

Fig. 7.3.4, with $\theta \to \phi$. Show that the associated potential is

$$\Phi = \frac{K_l d}{2\pi\sigma}\frac{\cos\phi}{r} \qquad (a)$$

in the limit $K_l \to \infty,\ d \to 0,\ K_l d$ finite.

7.4 Superposition and Uniqueness of Steady Conduction Solutions

7.4.1* A material of uniform conductivity has a spherical insulating cavity of radius b at its center. It is surrounded by segmented electrodes that are driven by current sources in such a way that at the spherical outer surface $r = a$, the radial current density is $J_r = -J_o\cos\theta$, where J_o is a given constant.

(a) Show that inside the conducting material, the potential is

$$\Phi = \frac{J_o b}{\sigma}\frac{\left[(r/b) + \frac{1}{2}(b/r)^2\right]}{\left[1 - (b/a)^3\right]}\cos\theta; \qquad b < r < a. \qquad (a)$$

(b) Evaluated at $r = b$, this gives the potential on the surface bounding the insulating cavity. Show that the potential in the cavity is

$$\Phi = \frac{3J_o}{2\sigma}\frac{r\cos\theta}{\left[1 - (b/a)^3\right]}; \qquad r < b \qquad (b)$$

7.4.2 A uniformly conducting material has a spherical interface at $r = a$, with a surrounding insulating material and a spherical boundary at $r = b$ $(b < a)$, where the radial current density is $J_r = J_o\cos\theta$, essentially independent of time.

(a) What is Φ in the conductor?
(b) What is Φ in the insulating region surrounding the conductor?

7.4.3 In a system that stretches to infinity in the $\pm x$ and $\pm z$ directions, there is a layer of uniformly conducting material having boundaries in the planes $y = 0$ and $y = -a$. The region $y > 0$ is free space, while a potential $\Phi = V\cos\beta x$ is imposed on the boundary at $y = -a$.

(a) Determine Φ in the conducting layer.
(b) What is Φ in the region $y > 0$?

7.4.4* The uniformly conducting material shown in cross-section in Fig. P7.4.4 extends to infinity in the $\pm z$ directions and has the shape of a 90-degree section from a circular cylindrical annulus. At $\phi = 0$ and $\phi = \pi/2$, it is in contact with grounded electrodes. The boundary at $r = a$ interfaces free

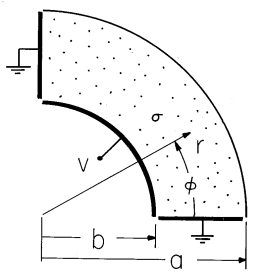

Fig. P7.4.4

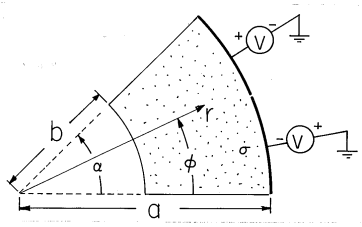

Fig. P7.4.5

space, while at $r = b$, an electrode constrains the potential to be v. Show that the potential in the conductor is

$$\Phi = \sum_{\substack{m=1 \\ \text{odd}}}^{\infty} \frac{4V}{m\pi} \frac{[(r/b)^{2m} + (a/b)^{4m}(b/r)^{2m}]}{[1 + (a/b)^{4m}]} \sin 2m\phi \qquad (a)$$

7.4.5 The cross-section of a uniformly conducting material that extends to infinity in the $\pm z$ directions is shown in Fig. P7.4.5. The boundaries at $r = b$, at $\phi = 0$, and at $\phi = \alpha$ interface insulating material. At $r = a$, voltage sources constrain $\Phi = -v/2$ over the range $0 < \phi < \alpha/2$, and $\Phi = v/2$ over the range $\alpha/2 < \phi < \alpha$.

(a) Find an infinite set of solutions for Φ that satisfy the boundary conditions at the three insulating surfaces.
(b) Determine Φ in the conductor.

7.4.6 The system of Fig. P7.4.4 is altered so that there is an electrode on the boundary at $r = a$. Determine the mutual conductance between this electrode and the one at $r = b$.

7.5 Steady Currents in Piece-Wise Uniform Conductors

7.5.1* A sphere having uniform conductivity σ_b is surrounded by material having the uniform conductivity σ_a. As shown in Fig. P7.5.1, electrodes at "infin-

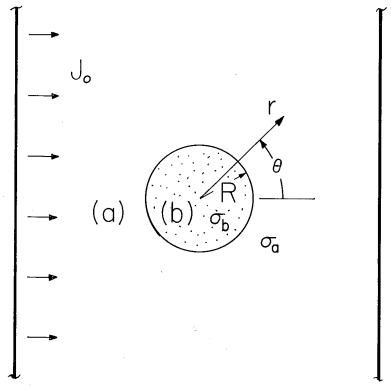

Fig. P7.5.1

ity" to the right and left impose a uniform current density J_o at infinity. Steady conduction prevails. Show that

$$\Phi = -\frac{J_o R}{\sigma_a} \begin{cases} \left[\frac{r}{R} + \left(\frac{\sigma_a - \sigma_b}{2\sigma_a + \sigma_b}\right)\left(\frac{R}{r}\right)^2\right]\cos\theta; & R < r \\ \left(\frac{3\sigma_a}{\sigma_b + 2\sigma_a}\right)\left(\frac{r}{R}\right)\cos\theta; & r < R \end{cases} \qquad (a)$$

7.5.2 Assume at the outset that the sphere of Prob. 7.5.1 is much more highly conducting than its surroundings.

(a) As far as the fields in region (a) are concerned, what is the boundary condition at $r = R$?
(b) Determine the approximate potential in region (a) and compare to the appropriate limiting potential from Prob. 7.5.1.
(c) Based on this potential in region (a), determine the approximate potential in the sphere and compare to the appropriate limit of Φ as found in Prob. 7.5.1.
(d) Now, assume that the sphere is much more insulating than its surroundings. Repeat the steps of parts (a)–(c).

7.5.3* A rectangular box having depth b, length l and width much larger than b has an insulating bottom and metallic ends which serve as electrodes. In Fig. P7.5.3a, the right electrode is extended upward and then back over the box. The box is filled to a depth b with a liquid having uniform conductivity. The region above is air. The voltage source can be regarded as imposing a potential in the plane $z = -l$ between the left and top electrodes that is linear.

(a) Show that the potential in the conductor is $\Phi = -vz/l$.
(b) In turn, show that in the region above the conductor, $\Phi = v(z/l)(x - a)/a$.
(c) What are the distributions of ρ_u and σ_u?

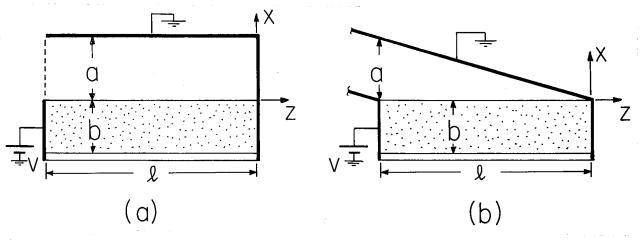

Fig. P7.5.3

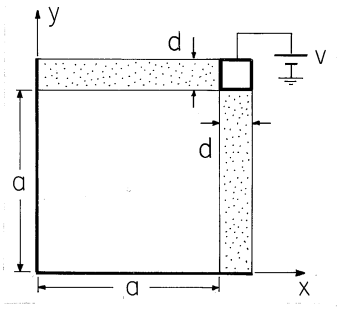

Fig. P7.5.4

(d) Now suppose that the upper electrode is slanted, as shown in Fig. P7.5.3b. Show that Φ in the conductor is unaltered but in the region between the conductor and the slanted plate, $\Phi = v[(z/l) + (x/a)]$.

7.5.4 The structure shown in Fig. P7.5.4 is infinite in the $\pm z$ directions. Each leg has the same uniform conductivity, and conduction is stationary. The walls in the x and in the y planes are perfectly conducting.

(a) Determine Φ, $\mathbf{E}$, and $\mathbf{J}$ in the conductors.
(b) What are Φ and $\mathbf{E}$ in the free space region?
(c) Sketch Φ and $\mathbf{E}$ in this region and in the conductors.

7.5.5 The system shown in cross-section by Fig. P7.5.6a extends to infinity in the $\pm x$ and $\pm z$ directions. The material of uniform conductivity σ_a to the right is bounded at $y = 0$ and $y = a$ by electrodes at zero potential. The material of uniform conductivity σ_b to the left is bounded in these planes by electrodes each at the potential v. The approach to finding the fields is similar to that used in Example 6.6.3.

(a) What is Φ^a as $x \to \infty$ and Φ^b as $x \to -\infty$?
(b) Add to each of these solutions an infinite set such that the boundary conditions are satisfied in the planes $y = 0$ and $y = a$ and as $x \to \pm\infty$.
(c) What two boundary conditions relate Φ^a to Φ^b in the plane $x = 0$?
(d) Use these conditions to determine the coefficients in the infinite series, and hence find Φ throughout the region between the electrodes.

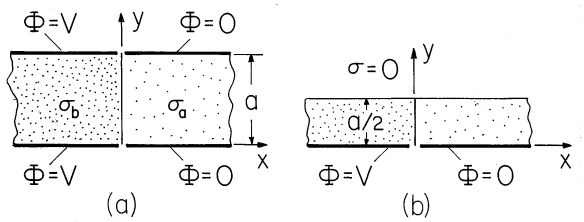

Fig. P7.5.5

(e) In the limits $\sigma_b \gg \sigma_a$ and $\sigma_b = \sigma_a$, sketch Φ and $\mathbf{E}$. (A numerical evaluation of the expressions for Φ is not required.)

(f) Shown in Fig. P7.5.6b is a similar system but with the conductors bounded from above by free space. Repeat the steps (a) through (e) for the fields in the conducting layer.

7.6 Conduction Analogs

7.6.1* In deducing (4) relating the capacitance of electrodes in an insulating material to the conductance of electrodes having the same shape in a conducting material, it is assumed that not only are the ratios of all dimensions in one situation the same as in the other (the systems are geometrically similar), but that the actual size of the two physical situations is the same. Show that if the systems are again geometrically similar but the length scale of the capacitor is l_ϵ while that of the conduction cell is l_σ, $RC = (\epsilon/\sigma)(l_\epsilon/l_\sigma)$.

7.7 Charge Relaxation in Uniform Conductors

7.7.1* In the two-dimensional configuration of Prob. 4.1.4, consider the field transient that results if the region within the cylinder of rectangular cross-section is filled by a material having uniform conductivity σ and permittivity ϵ.

(a) With the initial potential given by (a) of Prob. 4.1.4, with $\epsilon_o \rightarrow \epsilon$ and ρ_o a given constant, show that $\rho_u(x, y, t = 0)$ is given by (c) of Prob. 4.1.4.

(b) Show that for $t > 0$, ρ is given by (c) of Prob. 4.1.4 multiplied by $\exp(-t/\tau)$, where $\tau = \epsilon/\sigma$.

(c) Show that for $t > 0$, the potential is given by (a) of Prob. 4.1.4 multiplied by $\exp(-t/\tau)$.

(d) Show that for $t > 0$, the current $i(t)$ from the electrode segment is (f) of Prob. 4.1.4

7.7.2 When $t = 0$, the only net charge in a material having uniform σ and ϵ is the line charge of Prob. 4.5.4. As a function of time for $t > 0$, determine

the

(a) line charge density,
(b) charge density elsewhere in the medium, and
(c) the potential $\Phi(x, y, z, t)$.

7.7.3* When $t = 0$, the charged particle of Example 7.7.2 has a charge $q = q_o < -q_c$.

(a) Show that, as long as q remains less than $-q_c$, the net current to the particle is $i = -\frac{\mu\rho}{\epsilon}q$.
(b) Show that, as long as $q < -q_c$, $q = q_o \exp(-t/\tau_1)$ where $\tau_1 = \epsilon/\mu\rho$.

7.7.4 Relative to the potential at infinity on a plane passing through the equator of the particle in Example 7.7.2, what is the potential of the particle when its charge reaches $q = q_c$?

7.8 Electroquasistatic Conduction Laws for Inhomogeneous Materials

7.8.1* Use an approach similar to that illustrated in this section to show uniqueness of the solution to Poisson's equation for a given initial distribution of ρ and a given potential $\Phi = \Phi_\Sigma$ on the surface S', and a given current density $-(\sigma\nabla\Phi + \partial\epsilon\nabla\Phi/\partial t) \cdot \mathbf{n} = J_\Sigma$ on S'' where $S' + S''$ encloses the volume of interest V.

7.9 Charge Relaxation in Uniform and Piece-Wise Uniform Systems

7.9.1* We return to the coaxial circular cylindrical electrode configurations of Prob. 6.5.5. Now the material in region (2) of each has not only a uniform permittivity ϵ but a uniform conductivity σ as well. Given that $V(t) = Re\hat{V}\exp(j\omega t)$,

(a) show that $\mathbf{E}$ in the first configuration of Fig. P6.5.5 is $\mathbf{i_r}v/rln(a/b)$,
(b) while in the second configuration,

$$\mathbf{E} = \frac{\mathbf{i_r}}{r}Re\frac{\hat{v}}{Det}\begin{cases} j\omega\epsilon_o; & R < r < a \\ \sigma + j\omega\epsilon; & b < r < R \end{cases} \qquad (a)$$

where $Det = [\sigma\, ln(a/R)] + j\omega[\epsilon_o\, ln(R/b) + \epsilon ln(a/R)]$.
(c) Show that in the first configuration a length l (into the paper) is equivalent to a conductance G in parallel with a capacitance C where

$$G = \frac{[\sigma\alpha]l}{ln\,(a/b)}; \qquad C = \frac{[\epsilon_o(2\pi - \alpha) + \epsilon\alpha]l}{ln\,(a/b)} \qquad (b)$$

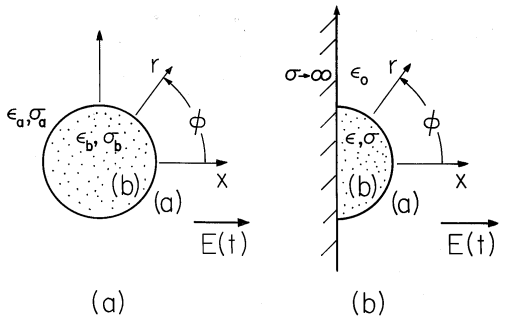

Fig. P7.9.4

while in the second, it is equivalent to the circuit of Fig. 7.9.5 with

$$G_a = 0; \qquad G_b = \frac{2\pi\sigma l}{ln\,(R/b)}$$

$$C_a = \frac{2\pi\epsilon_o l}{ln\,(a/R)}; \qquad C_b = \frac{2\pi\epsilon l}{ln\,(R/b)} \tag{c}$$

7.9.2 Interpret the configurations shown in Fig. P6.5.5 as spherical. An outer spherically shaped electrode has inside radius a, while an inner electrode positioned on the same center has radius b. Region (1) is free space while (2) has uniform ϵ and σ.

(a) For $V = V_o \cos(\omega t)$, determine $\mathbf{E}$ in each region.
(b) What are the elements in the equivalent circuit for each?

7.9.3* Show that the hemispherical electrode of Fig. 7.3.3 is equivalent to a circuit having a conductance $G = 2\pi\sigma a$ in parallel with a capacitance $C = 2\pi\epsilon a$.

7.9.4 The circular cylinder of Fig. P7.9.4a has ϵ_b and σ_b and is surrounded by material having ϵ_a and σ_a. The electric field $E(t)\mathbf{i_x}$ is applied at $x = \pm\infty$.

(a) Find the potential in and around the cylinder and the surface charge density that result from applying a step in field to a system that initially is free of charge.
(b) Find these quantities for the sinusoidal steady state response.
(c) Argue that these fields are equally applicable to the description of the configuration shown in Fig. P7.9.4b with the cylinder replaced by a half-cylinder on a perfectly conducting ground plane. In the limit where the exterior region is free space while the half-cylinder is so conducting that its charge relaxation time is short compared to times characterizing the applied field ($1/\omega$ in the sinusoidal steady state case), what are the approximate fields in the exterior and in the interior regions? (See Prob. 7.9.5 for a direct calculation of these approximate fields.)

7.9.5* The half-cylinder of Fig. P7.9.4b has a relaxation time that is short compared to times characterizing the applied field $E(t)$. The surrounding region is free space ($\sigma_a = 0$).

(a) Show that in the exterior region, the potential is approximately

$$\Phi^a \simeq -aE(t)\left[\frac{r}{a} - \frac{a}{r}\right]\cos\phi \qquad (a)$$

(b) In turn, show that the field inside the half-cylinder is approximately

$$\Phi^b \simeq -\frac{2\epsilon_o}{\sigma}\frac{dE}{dt}r\cos\phi \qquad (b)$$

7.9.6 An electric dipole having a z-directed moment $p(t)$ is situated at the origin and at the center of a spherical cavity of free space having a radius a in a material having uniform ϵ and σ. When $t < 0$, $p = 0$ and there is no charge anywhere. The dipole is a step function of time, instantaneously assuming a moment p_o when $t = 0$.

(a) An instant after the dipole is established, what is the distribution of Φ inside and outside the cavity?
(b) Long after the electric dipole is turned on and the fields have reached a steady state, what is the distribution of Φ?
(c) Determine $\Phi(r, \theta, t)$.

7.9.7* A planar layer of semi-insulating material has thickness d, uniform permittivity ϵ, and uniform conductivity σ, as shown in Fig. P7.9.7. From below it is bounded by contacting electrode segments that impose the potential $\Phi = V\cos\beta x$. The system extends to infinity in the $\pm x$ and $\pm z$ directions.

(a) The potential has been applied for a long time. Show that at $y = 0$, $\sigma_{su} = \epsilon_o V\beta\cos\beta x/\cosh\beta d$.
(b) When $t = 0$, the applied potential is turned off. Show that this unpaired surface charge density decays exponentially from the initial value from part (a) with the time constant $\tau = (\epsilon_o\tanh\beta d + \epsilon)/\sigma$.

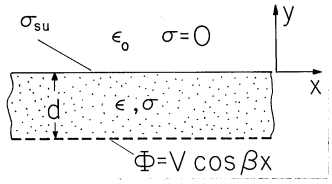

Fig. P7.9.7

7.9.8* Region (b), where $y < 0$, has uniform permittivity ϵ and conductivity σ, while region (a), where $0 < y$, is free space. Before $t = 0$ there are no

charges. When $t = 0$, a point charge Q is suddenly "turned on" at the location $(x, y, z) = (0, h, 0)$.

(a) Show that just after $t = 0$,

$$\Phi^a = \frac{Q}{4\pi\epsilon_o\sqrt{x^2 + (y-h)^2 + z^2}} - \frac{q_b}{4\pi\epsilon_o\sqrt{x^2 + (y+h)^2 + z^2}} \qquad (a)$$

$$\Phi^b = \frac{q_a}{4\pi\epsilon_o\sqrt{x^2 + (y-h)^2 + z^2}} \qquad (b)$$

where $q_b \to Q[(\epsilon/\epsilon_o) - 1]/[(\epsilon/\epsilon_o) + 1]$ and $q_a \to 2Q/[(\epsilon/\epsilon_o) + 1]$.

(b) Show that as $t \to \infty$, $q_b \to Q$ and the field in region (b) goes to zero.
(c) Show that the transient is described by (a) and (b) with

$$q_b = Q\left[1 - \left(\frac{2\epsilon_o}{\epsilon + \epsilon_o}\right)\exp(-t/\tau)\right] \qquad (c)$$

$$q_a = Q\left[\frac{2\epsilon_o}{(\epsilon + \epsilon_o)}\right]\exp(-t/\tau) \qquad (d)$$

where $\tau = (\epsilon_o + \epsilon)/\sigma$.

7.9.9* The cross-section of a two-dimensional system is shown in Fig. P7.9.9. The parallel plate capacitor to the left of the plane $x = 0$ extends to $x = -\infty$, with the lower electrode at potential $v(t)$ and the upper one grounded. This upper electrode extends to the right to the plane $x = b$, where it is bent downward to $y = 0$ and inward to the plane $x = 0$ along the surface $y = 0$. Region (a) is free space while region (b) to the left of the plane $x = 0$ has uniform permittivity ϵ and conductivity σ. The applied voltage $v(t)$ is a step function of magnitude V_o.

(a) The voltage has been on for a long-time. What are the field and potential distributions in region (b)? Having determined Φ^b, what is the potential in region (a)?
(b) Now, Φ is to be found for $t > 0$. Example 6.6.3 illustrates the approach that can be used. Show that in the limit $t \to \infty$, Φ becomes the result of part (a).
(c) In the special case where $\epsilon = \epsilon_o$, sketch the evolution of the field from the time just after the voltage is applied to the long-time limit of part (a).

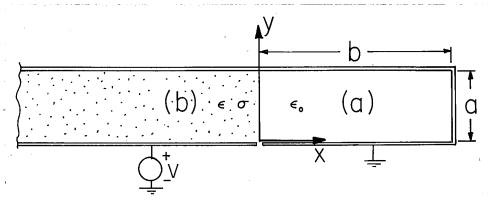

Fig. P7.9.9